Indoor Air

WILEY

SPECIAL ISSUE Emerging Digital Technologies and Trends for Enhancing Indoor Air Quality

RESEARCH ARTICLE OPEN ACCESS

IoT-Based Real-Time Monitoring Ecosystem on Smart Campus: Contributions for Infrastructure Deployment, CO_2-Based Ventilation, and Data-Driven Decisions

Ignacio Martínez | Enrique Cano | Álvaro Marco | Ángel Fernández

Human Openware Research Lab (HOWLab), Engineering Research Institute of Aragon (I3A), University of Zaragoza (UZ), Zaragoza, Spain

Correspondence: Ignacio Martínez (imr@unizar.es)

Received: 4 December 2025 | **Revised:** 12 March 2026 | **Accepted:** 2 April 2026

Guest Editor: Nima Izadyar

Keywords: CO_2 performance | data-driven decisions | indoor air quality (IAQ) | Internet of Things (IoT) | methodological framework

ABSTRACT

This paper addresses three indoor air quality (IAQ) challenges in large-scale infrastructures under real operational conditions. First, methodological procedures for CO_2 monitors: selection according to their key features, strategic placement to guarantee data quality, and calibration to ensure long-term consistency and second, real-time monitoring through a campus-scale Internet of Things (IoT) ecosystem, yielding the following contributions. A monitoring map is used to comprehensively classify spaces by fulfilling international recommendations. An IAQ study highlights the combined influence of occupancy, size, and contextual factors. And an analysis of CO_2 performance understands interactions between building operation and human behavior. Finally, for each contribution this paper proposes extrapolatable and replicable strategies to move toward data-driven decisions for efficient IAQ management in tertiary buildings.

Highlights

- Internet of Things (IoT)–driven strategies to understand carbon dioxide (CO_2) performance and enhance data-driven decisions.
- Methodological framework with reproducible procedures for selection, placement and calibration of CO_2 monitors.
- Monitoring map to identify critical situations, quantify IAQ variability, and select a representative set of study.
- IAQ study to highlight the combined influence of occupancy patterns, space size, and contextual factors.
- Analysis of CO_2 evolution by understanding interactions among building operation and human behavior.
- Contributions to IAQ complexity moving toward efficient IAQ management and planning in tertiary buildings.

1 | Introduction

Indoor air quality (IAQ) has become a central concern in building science, particularly since the COVID-19 pandemic [1], underscoring the relevance of enclosed spaces in airborne transmission. International agendas and regulatory frameworks converge on a common diagnosis: People spend 80%–90% of their time indoors, where pollutant concentrations and ventilation deficits frequently exceed recommended thresholds [2, 3]. Indoor environments accumulate pollutants of physical, chemical, and biological origin, generated by materials, equipment, infiltration, and human activity [4]. Among these pollutants, CO_2 occupies a specific diagnostic role; although not harmful at typical indoor levels, it is closely associated with occupancy and ventilation effectiveness and is widely used as an operational proxy for IAQ and for estimating the fraction of rebreathed air [5]. Thus, international standards [6–9] incorporate CO_2 as an indicator of the outdoor air supply relative to occupancy. Recent

global frameworks, including the United Nations Sustainable Development Goals (SDG) [10], have increasingly emphasized the role of healthy indoor environments in well-being and productivity. International reports [11–13] show that inadequate IAQ contributes to cognitive impairments, absenteeism, and increased risk of airborne transmission. Furthermore, postpandemic work [14] highlights the need for monitoring CO_2 levels, as a measurement of rebreathed air and a key indicator of the exposure risk in crowded indoor environments.

Educational buildings are particularly affected by these IAQ issues. A comprehensive literature review [15] underscores the importance of robust IAQ assessment strategies in tertiary buildings, particularly educational ones. CO_2 concentrations frequently exceed 1000–1500 ppm during teaching hours, especially under natural or mixed ventilation [16], but these educational environments are heterogeneous. Studies with multiroom monitoring in universities [17] reveal substantial heterogeneity between rooms of similar size and use, arising from differences in orientation, volume, performance, ventilation schedules, and user behavior. These findings show that IAQ performance varies significantly within the same building and often diverges from design expectations.

Beyond characterizing IAQ variability, the heterogeneity and complexity across buildings highlight a crucial point: The performance of tertiary buildings is intrinsically tied to their operating conditions. Franco et al. [18], through experimental analysis in a university campus under real operating conditions, characterize how similar spaces can show different CO_2 evolution patterns due to orientation, ventilation, and thermal inertia. By quantitatively analyzing an infection risk model applied to real classroom scenarios, Zivelonghi and Kumar [19] show how CO_2 behaviors vary across usage patterns (degrees, semesters, and exam periods), ventilation strategies (natural, mechanical, and mixed-mode systems), and architectural diversity (from compact north-facing classrooms to large- and high-inertia lecture theaters). These variations are difficult to anticipate during design and even harder to regulate through fixed ventilation rules, reinforcing the importance of empirical, long-term IAQ monitoring. Using a numerical simulation method to model CO_2 performance, Ren et al. [20] prove that the interaction between building typology, occupancy dynamics, and ventilation strategies produces high CO_2 variability. Spaces with similar layouts behave differently depending on their proximity to stairs or external façades, and organizational factors, such as timetabling practices and informal space use, further complicate predictions. This reinforces the need for methodologies capable of spatially and temporally capturing fine-scale variability. Notably, recent works [21] consider IAQ from a context-aware perspective and examine the interrelations among the built environment and its users while applying a smart approach. This Smart Built Environment (SBE) approach defines buildings as complex systems operating across seven interrelated fields: built environments, sensorized ecosystems, digital infrastructure, control and regulation systems, occupant behaviors, economic performance, and climate conditions.

In this context of heterogeneity and complexity, important methodological gaps remain. The literature seldom discusses explicit procedures for selecting monitors, evaluating detector technology, calibrating devices, and defining placement criteria [22]. Meanwhile, many works focus on IAQ monitoring under controlled or semicontrolled conditions [23]. These studies link CO_2 concentration with occupancy and ventilation rates, but are limited in scalability: Their gap with the real built environment does not specify how to deploy infrastructure containing a large number of spaces potentially to monitor (N) using a limited number of deployable sensors ($n \ll N$). Moreover, few works [24] evaluate the empirical heterogeneity of IAQ indicators and their interrelationships with contextual factors, such as orientation, location, size, occupancy, and window-opening patterns. This paper contributes to fill these knowledge gaps by addressing these three challenges: a lack of standardized procedures, a disparity between controlled experiments and real-world conditions, and insufficient correlation between IAQ indicators and multiple contextual factors.

Regarding the first challenge, few works deeply consider the methodological procedures used for selecting, placing, and calibrating CO_2 monitors, which represent a key preliminary step in building a verifiable dataset. Avila et al. [25] experimentally evaluate various natural ventilation strategies, finding that low-cost sensors, when correctly calibrated, provide reliable long-term IAQ assessment. Under real operating conditions in schools and universities, the COVID-19 pandemic revealed the prevalence of ventilation deficiencies during teaching hours. As Huang et al. [26] pose, site-specific monitoring systems are key to effectively assessing CO_2 behavior. A comprehensive literature review, as Marfo et al. [27] address, analyze 33 studies (from 432 full-text assessed articles), showing that guaranteeing data quality and validating CO_2 monitors are key challenges in deploying CO_2 monitoring ecosystems. At the same time, researchers are increasingly exploring data-driven predictive approaches for machine learning–based ventilation strategies, as Mousavi et al. [28] review, considering 451 recent research articles and 53 technical documents from American Society of Heating, Refrigerating and Air-Conditioning Enterprises (ASHRAE) handbooks. Notably, although these data-driven approaches show promising results, they typically assume that a monitored system is well characterized with well-placed sensors. In practice, this is a prior methodological step that is often insufficiently addressed: how many sensors to deploy, where to place them, and how to calibrate them systematically.

Regarding the second challenge, existing IAQ research largely relies on controlled or quasicontrolled conditions. Through laboratory experiments, tracer–gas studies, and simplified test rooms, Wei et al. [29] clarify fundamental relationships among occupancy, metabolic CO_2 generation, and ventilation under well-mixed conditions. By studying mechanical ventilation in 1 lecture theater, 2 open plan offices, 8 classrooms, and 14 meeting rooms, Oswin et al. [30] show that CO_2 levels reflect transient, spatially heterogeneous, and behavior-driven patterns. This contrast reflects the well-known building performance gap (BPG): predicted performance based on idealized assumptions rarely matches the complexities of real operation. Chenari et al. [31] investigate this gap with experimental research using a smart window equipped with mechanical ventilation boxes, occupancy sensors, and a real-time CO_2 monitoring system. Lu et al. [32] emphasize this gap by reviewing advances in the recent two decades in CO_2-based demand-controlled ventilation

in commercial buildings. However, these works often focus on a limited set of spaces, where the number of rooms to potentially monitor far exceeds the number of deployable sensors. Gao et al. [33], through a numerical study with computational fluid dynamics, highlight the need for continuous, in situ monitoring to understand how ventilation systems, architectural configurations, and occupant behavior interact under real conditions. Thus, to manage IAQ on a large-scale under real conditions, the rapid development of IoT and low-power wireless area network (LP-WAN) technologies become more urgent, expanding the possibilities for real-time monitoring. A systematic literature review, as Cimbru et al. [34] address by analyzing 56 academic and 18 practitioner studies, evidences that IoT-based systems enable continuous monitoring of CO_2 behavior to enhance risk prevention, real-time management, costs reduction, and energy efficiency. In educational buildings, digital approaches of IoT deployments, as Gasbarri et al. [35] propose and evaluate indoor environmental quality (IEQ) and user well-being in university buildings, providing support for decision-making in academic settings. Nevertheless, real-world implementations still face challenges, including interoperability issues, calibration drift, accurate representation, nonideal placement in complex geometries, and integration with building systems [36]. Building on these observations, recent studies [37, 38] emphasize how IoT infrastructures can support scalable and multibuilding sensing deployments. These works also show that LP-WAN technologies, such as low-range wireless area network (LoRaWAN), work well in educational campuses, where wireless fidelity (WiFi) technologies may be inconsistent or overloaded. The integration of real-time dashboards with cloud-based storage further supports not only real-time monitoring but also data-driven decisions-making and predictive modeling.

Regarding the third challenge, IAQ must be understood within the broader context of IEQ, necessitating a paradigm shift [39]. Although CO_2 alone cannot fully capture the concept of IEQ, it remains the most practical large-scale indicator for assessing ventilation. Its interpretability, cost-efficiency, and compatibility with context-aware IoT solutions make it suitable for multibuilding studies [40]. In this context, digital-twin technologies are increasingly adopted among smart-campus initiatives, enabling cross-layer data integration and coordinating responses to IAQ issues across departments. This digital integration creates new opportunities for occupancy analytics, energy management, data-driven maintenance, adaptive control, and long-term optimization [41]. Many postpandemic works analyze IEQ in real educational buildings, but provide aggregated indicators. Franco et al. [42] employ different occupancy models in public buildings and shows that CO_2 monitoring strengthens IAQ management by guiding the heating, ventilation, and air conditioning (HVAC) operations based on occupancy and environmental conditions. However, university campuses are large and heterogeneous. Although their CO_2 dynamics depend on occupancy rhythms, architectural configurations, ventilation strategies, user behaviors, and multiple contextual factors, few works discuss the cross-correlation dependences following a systematic methodology [43]. This reinforces the need for a methodological framework capable of handling contextual variability and real-world complexity.

Within this broader context, this paper addresses these challenges following the research framework illustrated in Figure 1, deployed on the University of Zaragoza smart campus [44]. The three major contributions of this work are outlined as follows:

- Methodological procedures, detailed in Section 2, for (2.1) selecting CO_2 monitors according to their key features; (2.2) determining placement strategies across representative classroom types; and (2.3) calibrating devices to ensure long-term consistency and comparability. As a result, this

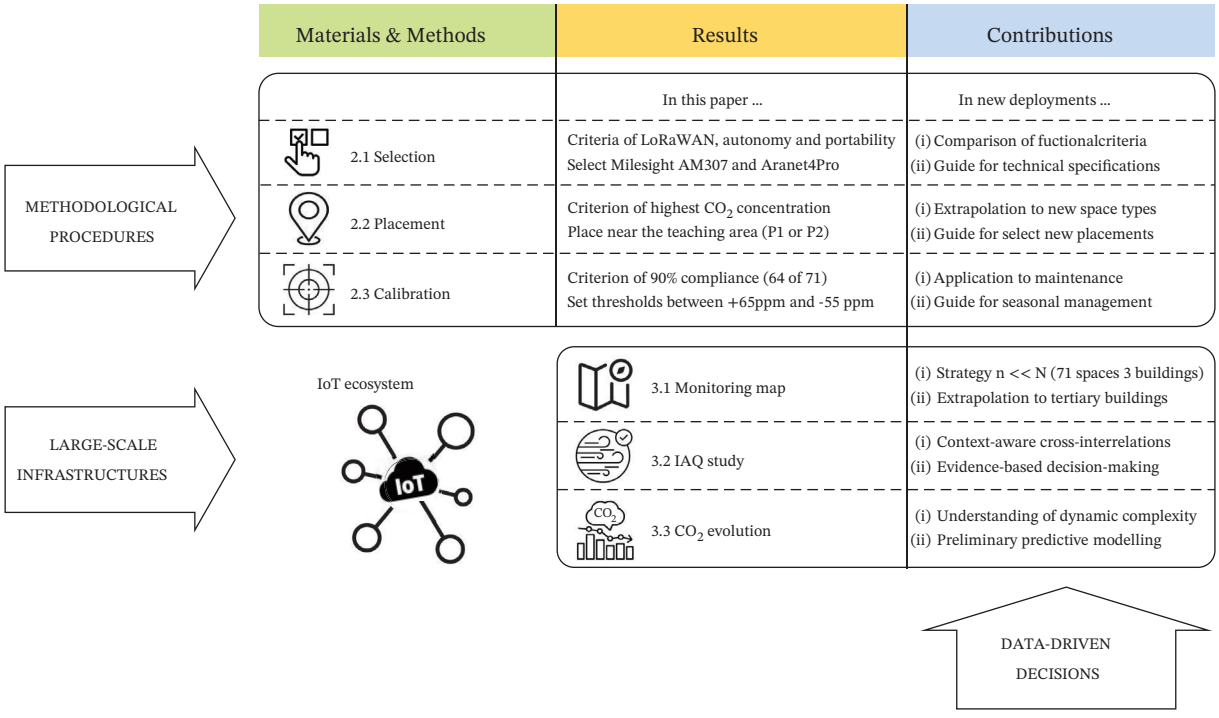

FIGURE 1 | Research framework.

paper shows the criteria followed to fulfill the international recommendations. And, for new deployments, we propose several guides (as a practical and replicable strategy) to extrapolate these results to heterogeneous educational environments with other types of spaces, new placements, seasonal maintenance, etc.

- Large-scale infrastructure, detailed in Section 3, with three types of approaches: (3.1) a campus-wide monitoring map to identify critical situations (CO_2 above 1500 ppm), quantify IAQ variability, and select a representative subset of n spaces from the total N locations (to allow relocating sensors according to a $n \ll N$ strategy); (3.2) an IAQ study that includes an evaluation of the air pollutants and a CO_2 cross-analysis by highlighting the combined influence of occupancy patterns, space size and contextual factors; and (3.3) an analysis of CO_2 evolution by understanding interactions among building operation and human behavior.
- Data-driven decisions, as actionable strategies proposed as contributions, for each type of approach: classification of representative spaces under real conditions to extrapolate to tertiary buildings; evidence-based decision-making through context-aware interrelations; and preliminary predictive modeling to understand the complexity of CO_2 behavior considering multiple factors: orientation, location, size, occupancy, user behavior, seasonal variations, types of days, and ventilation strategies.

These contributions align with this *Special Issue* by demonstrating how IoT-driven initiatives within context-aware analyses enable more informed and efficient IAQ decisions in complex educational environments.

2 | Materials and Methods

As outlined in the Introduction, this paper addresses the challenge to develop an IoT real-time monitoring ecosystem in a heterogeneous smart campus environment. Buildings differ in orientation, occupancy patterns, ventilation behavior, and HVAC operation, among other factors. Thus, IoT deployment requires a methodological framework. Furthermore, the monitoring strategy must be efficient, relocatable, scalable, and reproducible: The smart campus must monitor N spaces but costs, investments and logistics recommend deploying only n ($n \ll N$) sensors. For these reasons, this paper proposes a three-stage methodology for CO_2 monitor deployment: (a) selection according to their key features (detector technology, calibration, connectivity, screen, autonomy, and price), (b) placement based on the spatial configuration and use of each space type, and (c) calibration using a sequenced and reproducible procedure. The following subsections describe these stages and the specific challenges addressed in each of them.

2.1 | Selection of CO_2 Monitors

Indoor CO_2 can be measured using different sensing principles [45], but nondispersive infrared (NDIR) detectors remain the most reliable option for long-term IAQ assessment in real buildings [46]. NDIR sensors quantify CO_2 concentration by measuring infrared absorption within a sealed gas chamber (see an operating diagram in Figure 2), a technique with well-documented stability and robustness for continuous monitoring. Commercial detectors [47] vary in measurement range, uncertainty, response time, and expected lifetime (see Table 1). These specifications, along with calibration behavior and connectivity requirements, directly influence the validity of the dataset in campus-scale deployments.

In heterogeneous tertiary buildings, such as the smart campus considered in this study, the monitoring infrastructure must satisfy several constraints. The number of spaces to potentially monitor is large (in this study, $N = 71$ across 3 buildings). The number of deployable sensors must remain limited ($n \ll N$, in this study $n = 15$) owing to financial and logistical factors. CO_2 monitors must operate continuously and comparably across buildings with different orientations, uses, and HVAC configurations. Measurements must remain stable over months despite calibration drift, variable environmental conditions, and differences in local airflow patterns. For these reasons, the selection process must prioritize functional and methodological criteria rather than device-specific characteristics. With these premises, this paper considers the following key criteria, highlighting the CO_2 monitors that best fit each criterion in Table 2.

The initial criterion is detector technology and calibration. NDIR detectors differ substantially in how they maintain their reference baseline: Some offer daily automatic baseline correction

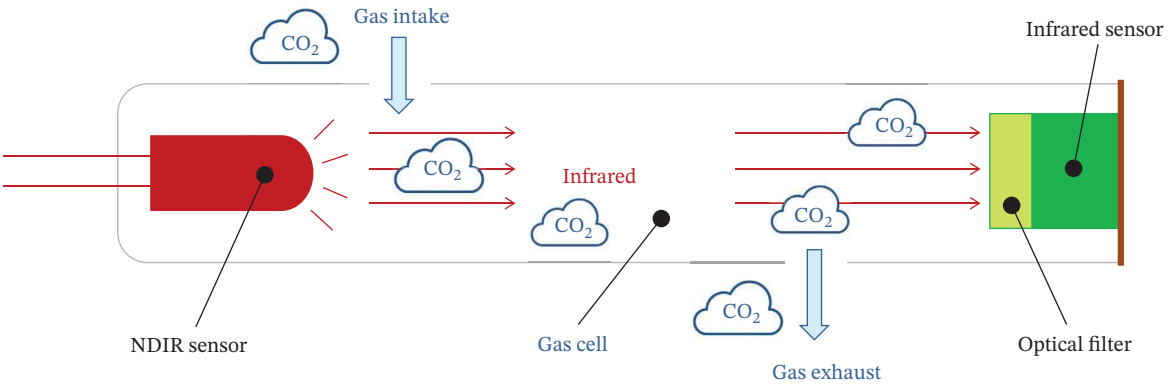

FIGURE 2 | NDIR sensor: operating diagram.

TABLE 1 | NDIR detectors; technical specifications.

				
NDIR detector	MH-Z19B	SenseAir S8	SenseAir Sunrise	CozIR-LP
Measurement interval (ppm)	0–5000	0–2000 (indoor) 0–10000 (outdoor)	400–10000	400–5000
Uncertainty	± 50 ppm or ± 5% measurement	± 50 ppm or ± 3% measurement	± 30 ppm or ± 3% measurement	±30 ppm or ± 3% measurement
Response time (s)	< 120	120	16	30
Useful life (years)	> 5	> 15	> 15	> 5

TABLE 2 | CO_2 monitors: criteria comparison.

CO_2 monitor		CO_2 detector	Calibration	Connectivity	Autonomy	Screen	Price
	SanityAir [48]	CozIR-LP	No	No	Cable	Yes	€150–€200
	Milesight AM307/308/319 [49]	CozIR-LP	Automatic (manual option)	LoRaWAN	3 years (AA batteries)	Yes	€150–€200
	Aranet4 Home/ Pro [50]	SenseAir Sunrise	Automatic (manual option)	Bluetooth LoRaWAN	2 years (AA batteries)	Yes	€200–€250
	DM 72C/1306/1307 [51]	SenseAir S8	No	No	Cable	Yes (big screen)	€150–€200
	CO_2 panel PI/ matrix [52]	MH-Z19B	Manual	WiFi downloadable data	Cable	No (led light)	€100–€150
	Dioxcare [53]	SenseAir S8	Manual	USB downloadable data	14-h rechargeable battery (cable)	Yes	€50–€100

(e.g., MH-Z19B), whereas others guarantee monthly drift below 10% (e.g., SenseAir S8), and more advanced detectors implement weekly auto-calibration combined with the option for manual reference adjustment (e.g., SenseAir Sunrise and CozIR-LP). As the subsequent IAQ analysis depends on comparing measurements across multiple spaces and buildings, long-term calibration stability became essential.

The next key criterion is connectivity, considering that a main objective is to collect real-time data continuously without manual data retrieval. Thus, this criterion excludes CO_2 monitors without remote communication or requiring periodic downloads. Since the smart campus IoT ecosystem already incorporates LoRaWAN gateways, this paper prioritizes CO_2 monitors compatible with this technology, leveraging their indoor range, ubiquitous connectivity, widespread adoption, low power consumption, and seamless integration with existing infrastructure [54].

Another key criterion is autonomy, to support multimonth studies and redeployment. This implies ubiquity, understood as the ability to relocate CO_2 monitors across representative spaces according to the $n \ll N$ strategy, as well as comparability to ensure that measurements from different detectors can be interpreted consistently.

Although not central to data acquisition, screen characteristics determine the visual feedback, which can influence user perception and space usage. However, this paper deprioritizes CO_2 monitors designed primarily for local display because they

typically lack connectivity and therefore limit scalability in a distributed IoT ecosystem.

Finally, price is an important criterion to consider, for achieving cost–functionality balance. The need to monitor many spaces means that the unit price cannot be considered independently of autonomy, calibration and connectivity. Low-price CO_2 monitors are useful only when they meet these requirements, whereas high-performance CO_2 monitors without connectivity or with limited autonomy impose hidden operational costs.

Based on these criteria, and after analyzing several commercially available devices (see Table 2), we select two CO_2 monitors: Milesight AM307, incorporating a CozIR-LP detector; and Aranet4 Pro, based on the SenseAir Sunrise detector. These devices combine reliable NDIR detection, robust calibration behavior, LoRaWAN connectivity, long autonomy (over 2 years), and full portability. Using two sensor technologies also increases methodological robustness by enabling cross-comparison of the measurements under real operating conditions. This selection ensures consistent, interoperable, and scalable data acquisition across heterogeneous indoor environments, as a basis for the subsequent space-classification methodology and IAQ analysis. Moreover, the portability, autonomy, and connectivity of these selected CO_2 monitors allow the methodology to be replicated in other buildings, locations, and contexts without increasing infrastructure costs.

2.2 | Placement of CO_2 Monitors

With the CO_2 monitors selected, the next step is to determine their optimal placement within each indoor space. As Introduction states, CO_2 distribution in real buildings strongly depends on contextual factors such as space geometry, ventilation pathways, façade orientation, HVAC operation, and occupant behavior. These contextual boundary conditions require an evaluation of the key features of each space: orientation, windows and doors (number, size, and location), layout (teacher and seating areas), etc. Following this methodology, this paper chooses the optimal placements and proposes their extrapolation to other types of space.

Identifying the most critical measurement points is essential to ensure meaningful long-term monitoring. This criterion of the most critical placement corresponds to the location where the CO_2 concentration is highest. Since these locations depend on the space typology, all the spaces across the smart campus follow two recurrent configurations (see Figure 3). Type A shows a lateral window façade parallel to the seating and teaching areas and a door typically located on the wall opposite the windows. Type B shows a windows area at the back of the space opposite the teaching area and doors near the teaching area. Since these geometries influence airflow patterns, fresh-air entry, and potential CO_2 accumulation zones, it is necessary to recontextualize this placement analysis for each researching study.

Thus, to determine the optimal placements, we perform a situational analysis in each space (Types A and B), evaluating five points (P1–P5) with the highest potential CO_2 concentrations. We select these points according to the expected airflow, proximity to doors and windows, and anticipated sources of exhaled CO_2. Figure 4 depicts the proposed placement scheme and Table 3 describes each placement.

The placement study follows real teaching conditions to ensure that the measurements reflect genuine IAQ behavior rather than idealized or laboratory-like scenarios. To this end, we deliberately reproduce the following operational conditions (extrapolated for each specific context):

- The space is fully occupied at medium-to-high density. This ensures that the CO_2 concentration is sufficiently high to reveal the highest CO_2 accumulation zones for CO_2 monitor placement.
- The HVAC system operates under its normal schedule. When CO_2 concentrations rise, we partially open the windows so that natural ventilation complements mechanical ventilation, reproducing realistic mixed-mode operation.
- The entrance doors remain open for approximately 10 min at the start of the class and are then closed for the remainder of the session. This reproduces standard teaching practice and allows for observation of the door-driven air exchange.
- Windows opening follows the typical behavior of each space (closed, partially open, or fully open), reflecting the real variability based on orientation, weather conditions, and user habits.
- CO_2 monitors recalibrate their sensors (in clean air) for 10 min before measurements begin. Then, monitors record the CO_2 concentration (in parts per million [ppm]) over a 60-min teaching session in four consecutive 15-min intervals. This procedure enables identification of the locations with the highest and most persistent CO_2 levels.

(a) (b)

FIGURE 3 | Space configurations in the smart campus: (a) Type A and (b) Type B.

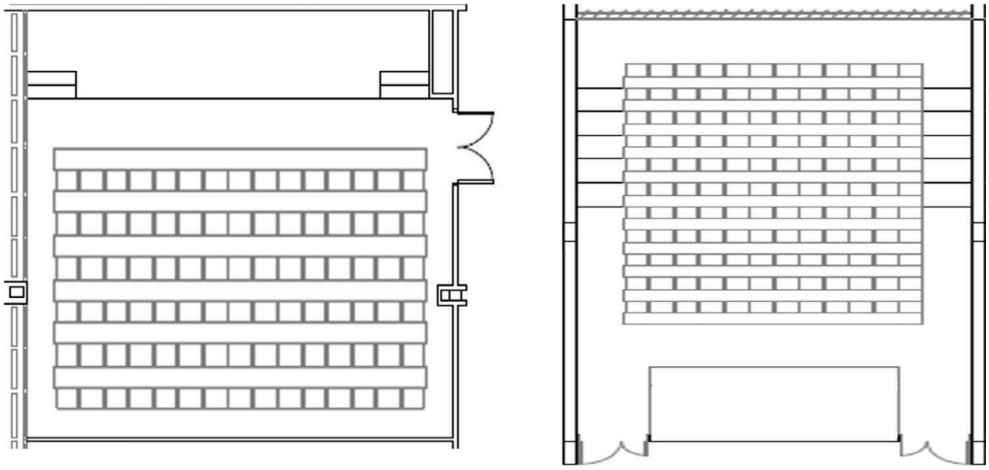

(a) (b)

FIGURE 4 | CO_2 monitors. Placement scheme: (a) Type A and (b) Type B.

TABLE 3 | Placement description.

Placement	Type A	Type B
P1	Near corner at teaching area (closed window)	Near corner at teaching area (closed doors)
P2	Far corner at teaching area (initially with open door)	Far corner at teaching area (initially with open door)
P3	In front of the door (initially with open door)	In front of the door (initially with open door)
P4	In the center of the seating area	In the center of the seating area
P5	Back corner (opposite the door)	Back corner and close to windows area (partially open)

The results (see Tables 4 and 5) show that, in both Types A and B, the highest CO_2 concentrations consistently occurred near the teaching area (P1 or P2). In Type A spaces, Table 4 indicates that the most unfavorable measurements appear in P1, where values highlight the highest CO_2 concentration near the teacher area. This is consistent with the fact that the teacher speaks continuously during teaching, expending more energy and potentially generating more exhaled CO_2. This effect is even more pronounced when the window located near that corner is closed, which restricts ventilation. When that window is open, P2 (far corner in the teaching area) becomes the recommended placement because it remains away from fresh-air inflow while still capturing the teacher-driven CO_2 rise.

In Type B spaces, Table 5 shows that P1 again exhibits the highest CO_2 concentrations, due to limited airflow in the teaching area and continuous exhalation by theteacher. In these spaces, without windows near the teaching area and closed doors during class, P2 captures measurements similar to P1 and is therefore the second most optimal placement with highest CO_2 levels. These areas are characterized by limited airflow and continuous exhalation from the teacher, making them the placement choice for long-term monitoring. Locations near the door (P3) or central seating areas (P4) show lower CO_2 concentrations due to higher mixing and airflow, whereas back-corner behavior (P5) depends on window operation and façade orientation.

To validate with statistical rigor the selection of P1 placement, a statistical analysis is conducted. This analysis seeks convergence (toward the best placement), stability (to ensure statistically significance), and superiority (over other alternatives). As placements are space-dependent, we separately perform all analyses for Types A and B. Given that the sample size is four timestamps per hour (in five comparative placements) with a non-normal distribution of the data, we suggest applying non-parametric statistical tests.

The Friedman test assesses if the placements (P1–P5) show global differences across the four timestamps. As an expected result, Friedman test sets that CO_2 measurements significantly change their levels if $p < 0.05$. As shown in Table 6 for both Types A and B, test results reveal statistically significant differences, with $p = 0.0039$ (Type A) and $p = 0.0042$ (Type B). These results confirm that CO_2 measurements strongly depend on the monitor placement, with very large effect sizes (Kendall's $W > 0.95$) and high consistency ($X^2 > 15$).

To further examine whether P1 systematically captures the highest CO_2 concentrations, Wilcoxon signed-rank tests compare P1 against each alternative position (P2–P5). As shown in Table 7, P1 consistently exhibits the highest CO_2 levels across all timeslots and both Types A and B. Pairwise comparisons confirm the consistency, with the statistic $W = 10.0$ ($W = 6.0$ for P2 in Type B).

Empirically data-supported, taken together the statistically significant global differences, the large effect sizes, and the consistent ranking of P1 support its selection as the standard placement criteria for all spaces and both types A and B.

TABLE 4 | CO_2 measurements: Type A.

	Measurement #1		Measurement #2		Measurement #3		Measurement #4	
Placement	Timeslot (minutes)	CO_2 (ppm)	Timeslot (minutes)	CO_2 (ppm)	Timeslot (minutes)	CO_2 (ppm)	Timeslot (minutes)	CO_2 (ppm)
P1	00–15	532	15–30	539	30–45	522	45–60	559
P2	00–15	522	15–30	510	30–45	517	45–60	539
P3	00–15	479	15–30	486	30–45	478	45–60	520
P4	00–15	521	15–30	498	30–45	495	45–60	530
P5	00–15	501	15–30	500	30–45	505	45–60	533

TABLE 5 | CO_2 measurements: Type B.

	Measurement #1		Measurement #2		Measurement #3		Measurement #4	
Placement	Timeslot (minutes)	CO_2 (ppm)	Timeslot (minutes)	CO_2 (ppm)	Timeslot (minutes)	CO_2 (ppm)	Timeslot (minutes)	CO_2 (ppm)
P1	00–15	504	15–30	498	30–45	505	45–60	491
P2	00–15	490	15–30	498	30–45	491	45–60	488
P3	00–15	472	15–30	469	30–45	476	45–60	461
P4	00–15	473	15–30	493	30–45	489	45–60	487
P5	00–15	471	15–30	479	30–45	482	45–60	473

TABLE 6 | Friedman test for P1–P5 placements.

	X^2	p	Kendall's W
Type A	15.40	0.0039	0.96
Type B	15.24	0.0042	0.95

To extrapolate this methodology to other architectural typologies (e.g., open plan offices, laboratories, auditoriums, complex spaces, etc.), this paper proposes the following procedure:

- Draw the space layout and, similar to Figure 4, highlight its key areas: windows and doors, main areas where people conduct energetic activities (e.g., working, walking and talking), and secondary areas where people conduct nonenergetic activities (e.g., listening, watching, and working in silence).
- Identify several points (P1–P5 in this paper) with potentially the highest CO_2 concentrations.
- Reproduce the operational conditions (teaching and learning in this paper) for each specific context.
- Monitor the CO_2 measurements (Tables 4 and 5) at each identified point (P1–P5) of highest CO_2 levels.
- Apply statistical significance analysis (as Friedman test and Wilcoxon signed-rank tests) to ensure convergence, stability, and superiority in the selection of the optimal placement (P1 in this paper). Additionally, choose a secondary placement option (P2 in this paper) as an operational alternative.

TABLE 7 | Wilcoxon signed-rank tests for P1 against P2–P5 placements.

	W	p	r	p_holm
		(a) Type A		
P2	10.0	0.0625	0.7670	0.25
P3	10.0	0.0625	0.7670	0.25
P4	10.0	0.0625	0.7670	0.25
P5	10.0	0.0625	0.7670	0.25
		(b) Type B		
P2	6.0	0.1250	0.5751	0.25
P3	10.0	0.0625	0.7670	0.25
P4	10.0	0.0625	0.7670	0.25
P5	10.0	0.0625	0.7670	0.25

After determining the optimal location, we deploy CO_2 monitors across all spaces to potentially monitor (see Figure 5 for the full campus-wide deployment map with 71 locations in 3 buildings: A, B, and C), following a consistent nomenclature. The deployment of the two previously selected types of CO_2 monitors (Milesight AM307 and Aranet4 Pro) alternates between spaces to ensure comparability across building orientations and space configurations.

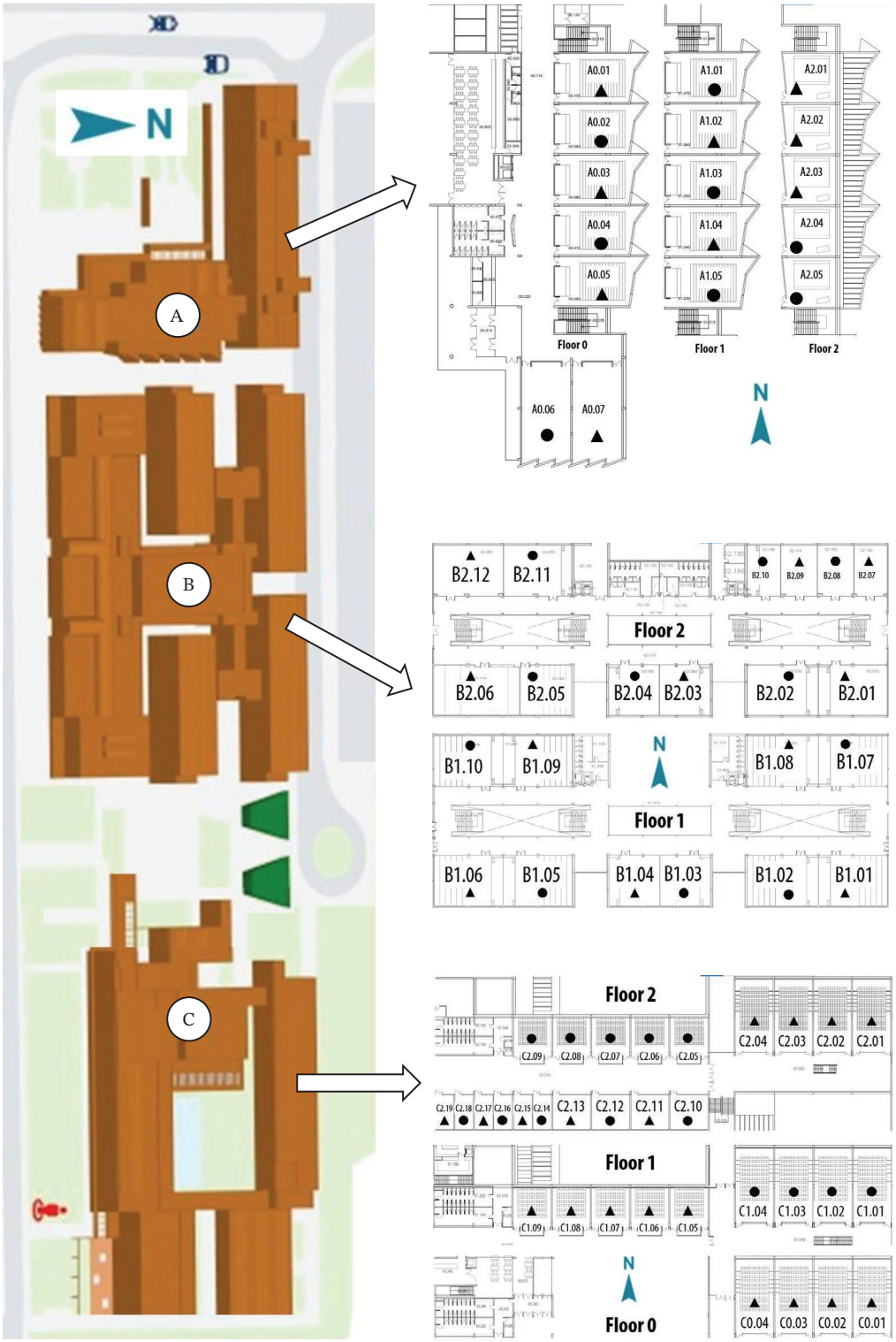

FIGURE 5 | Campus-wide deployment map. The figure includes (i) nomenclature to identify each monitored space (building = A / B / C, floor = 0 / 1 / 2, and space identifier = 01 / 02 / ..), (ii) sensor-type markers (circle = Milesight AM307, and triangle = Aranet4 Pro), and (iii) a compass icon to indicate building orientation.

2.3 | Calibration of CO_2 Monitors

With the CO_2 monitors deployed across the three buildings of the smart campus, and prior to collecting operational data, it is necessary to carry out a calibration procedure. This calibration procedure is aimed at establishing a criterion to determinate whether each CO_2 monitor operates correctly or requires calibration. A key point in this procedure is understanding that measurements obtained from a CO_2 monitor may be either above or below the real CO_2 concentration. If a monitor underestimates the CO_2 level, the real concentration would be higher than the measurement. It implies that the space would appear

to be sufficiently ventilated when it is not, which could lead to insufficient ventilation and, therefore, lower IAQ levels, potentially compromising occupants' health. Conversely, if a monitor overestimates the real CO_2 level, subsequent overventilation is acceptable, as it leads to improve IAQ conditions. For this reason, the calibration procedure must be more restrictive with measurements that are below the real concentration.

To determine an acceptable error margin and verify the proper performance of the deployed CO_2 monitors, this paper proposes the following sequenced calibration procedure:

1. Obtain reference CO_2 measurements using a certified device: This study uses the Testo 480 monitor [55] with a calibration certificate.
2. Obtain CO_2 measurements for each monitored location, using the deployed CO_2 monitors.
3. Compute the difference between obtained CO_2 measurements and the certified reference: Figure 6 shows these differences (in ppm, vertical axis) for all monitored spaces in Buildings A, B, and C, grouped by floor.
4. Analyze the dispersion of the obtained CO_2 measurements in order to determine the upper and lower thresholds that indicate whether each CO_2 monitor is properly measuring or requires calibration; To establish these thresholds, this paper proposes the following criterion:

- Take as an initial reference the uncertainty specified for NDIR detectors (see Table 1), which ranges between ±3% and ±5% measurement or ±30 and ±50 ppm.
- Calculate the uncertainty levels: Using all CO_2 measurements collected herein, the mean value obtained is 502 ppm. Thus, the uncertainty levels corresponding to this mean value are ±15.06 ppm (±3%) or ±25.10 ppm (±5%), and alternatively, ±30 ppm or ±50 ppm, as specified by NDIR manufacturers.
- Quantify the percentage of CO_2 measurements that meet each uncertainty level: Figure 6 (horizontal dotted lines) indicates the following compliance levels: 30% (21 of 71 measurements) for ±15 ppm, 46% (33 of 71) for ±25 ppm, 53% (38 of 71) for ±30 ppm, and 80% (57 of 71) for ±50 ppm.

5. Choose the compliance level: Considering the number of deployed CO_2 monitors, the associated calibration costs (according to infrastructures, operatives, etc.), and the magnitude of acceptable error (in absolute value), this paper targets a 90% compliance (this choice could be adjusted for each specific context). With this compliance level of 90% (64 of 71 measurements), thresholds are set (see Figure 6) at +65 ppm (upper, red line) and −55 ppm (lower, blue line).
6. Calibrate the CO_2 monitors exceeding the target thresholds: Under this 90% compliance level, only seven CO_2 monitors require calibration (Locations B1.07, B2.05, C0.01, C0.04, C1.05, C2.06, and C2.13).

This procedure means the initial calibration before deployment. To validate the durability of this calibration procedure, the long-term sensor stability, and potential seasonal variations across a full year must be considered, which govern the need for periodic recalibration. In tertiary and institutional buildings, long-term maintenance involves multiple costs (human and material), logistical and operating factors, planning, routine monitoring, among others. However, in this context of CO_2 measuring, the behavior of CO_2 helps with its recalibration. Without occupancy or activity, the CO_2 levels reduce to their reference baseline around 420 ppm. As discussed in Section 3.3. by analyzing the day-by-day CO_2 evolution, the CO_2 measurements during weekends verify that the CO_2 monitors remain calibrated. In this paper, the recalibration criterion sets the same thresholds determined for initial calibration: +65 ppm and −55 ppm relative to the CO_2 baseline of 420 ppm. Thus, a CO_2 monitor is recalibrated when it does not meet this criterion for three weekends in a month. Table 8 reports monthly drift rates across a full yearand highlights the recalibration points when weekend CO_2 measurements do not fulfill the thresholds. These statistics show how this automated check procedure by monitoring the weekend CO_2 baseline leads a sustainable and cost-effective intervention for long-term maintenance of the deployed infrastructure.

To confirm the statistical significance of this procedure, the paired Wilcoxon signed-rank test reveals a very small shift ($p < 0.001$). For each building across a full year, Figure 7 shows how the mean drifts rates are ±24 ppm (dashed blue line), with 95% of the CO_2 monitors fulfilling the calibration thresholds. This homogeneous behavior across buildings, with a lack of progressive divergence, indicating that the CO_2 monitors remain stable. Hence, following these calibration and recalibration procedures, all CO_2 monitors are ready for accurate long-term IAQ monitoring across the smart campus.

3 | Results

From the previously proposed methodology, this section analyzes the results obtained to propose three types of contributions that support informed decision-making for efficient IAQ management and planning:

- A monitoring map, providing a complete overview of the CO_2 levels across the smart campus. This map enables (a) global quantification of the IAQ levels, (b) categorization of all spaces according to their IAQ performance, and (c) identification of a subset of representative spaces for their subsequent IAQ study.
- An IAQ study focused on these representative spaces, examining the relationships between IAQ behavior and key contextual factors that characterize each space type: orientation, location, size, and occupancy.
- An analysis of CO_2 evolution, presented through two complementary visualizations (day-by-day and hour-by-hour), elucidating the CO_2 dynamics in relation to working and non-working days, holiday periods, HVAC operation, and natural ventilation processes (such as window and door opening).

These three analytical layers provide a coherent framework for understanding IAQ behavior in heterogeneous educational buildings and for supporting data-driven ventilation and space-management strategies.

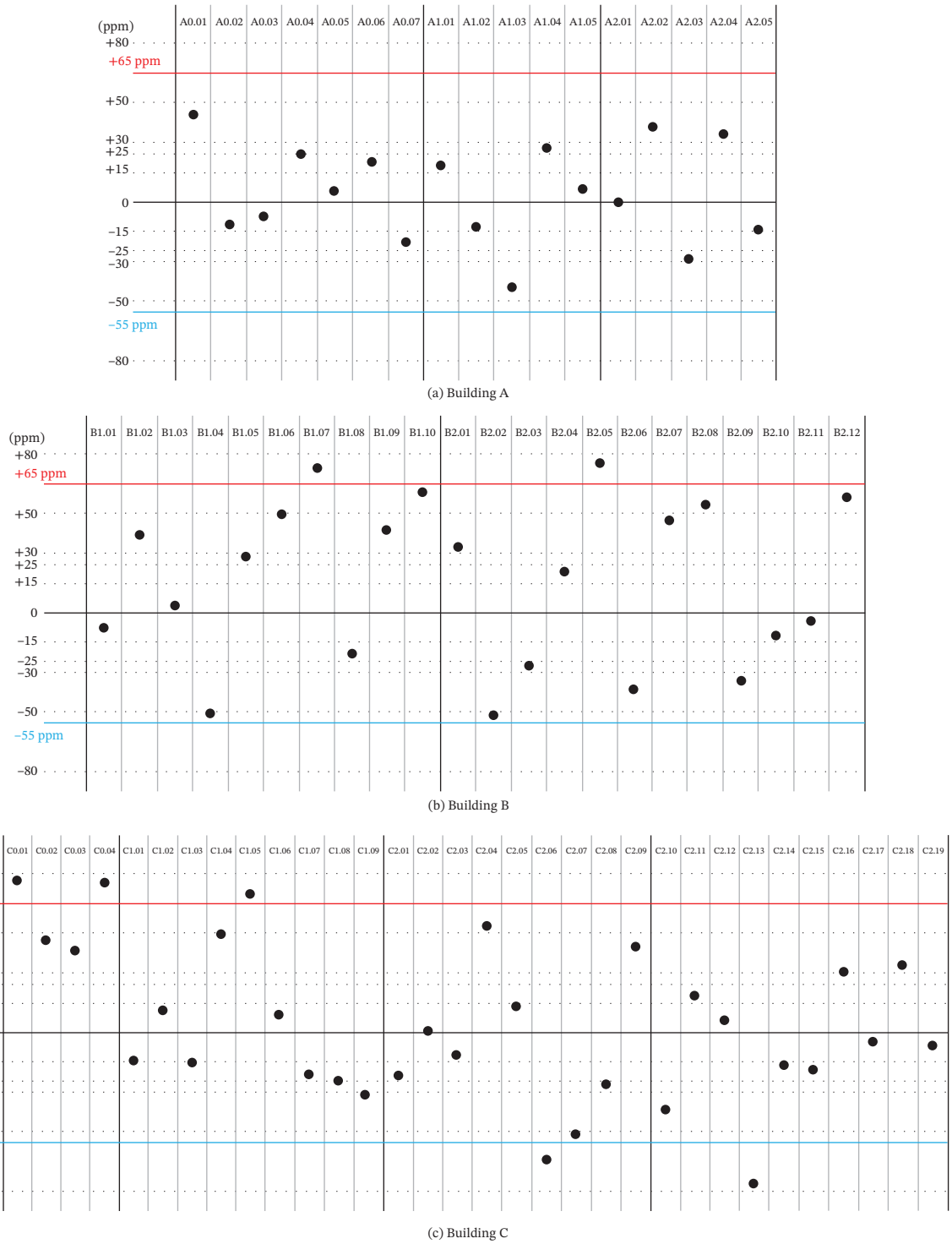

FIGURE 6 | Calibration procedure: differences in CO_2 measurements between the certified reference device and the deployed CO_2 monitors.

3.1 | Monitoring Map

The monitoring map constitutes the starting point for analyzing IAQ behavior across the smart campus. Its purpose is to offer a coherent, campus-wide overview of CO_2 conditions under real operating contexts, enabling comparisons between buildings, floors, and space types. From this map, the subsequent identification of representative spaces helps understand the heterogeneity, as highlighted in the Introduction. To generate this map, the dataset structures the diversity of IAQ performance across the smart campus. Herein, the monitoring procedure involves the following steps:

- Obtain CO_2 data as real-time measurements through the deployed IoT ecosystem from 71 locations (see Figure 5): 17 in Building A (7 on Floor 0, 5 on Floor 1, and 5 on Floor 2), 22 in Building B (10 on Floor 1 and 12 on Floor 2), and 32 in Building C (4 on Floor 0, 9 on Floor 1, and 19 on Floor 2).

TABLE 8 | Monthly drift rates relative to the CO_2 baseline for the recalibration check.

	Sep	Oct	Nov	Dec	Jan	Feb	Mar	Apr	May	Jun	Jul	Aug
(a) Building A												
A0.01	−2	+5	+12	+8	+5	+2	+0	−2	+2	0	−8	−15
A0.02	+15	+12	+22	+28	+45	+52	+60	+78	+20	+18	+5	−2
A0.03	+42	+55	+60	+62	+59	+42	+75	+25	+15	+12	−8	−18
A0.04	−5	0	+8	+5	+2	0	−2	−5	−2	−5	−8	−12
A0.05	+8	+15	+22	+18	+18	+15	+12	+10	+12	+10	+2	−2
A0.06	+55	+57	+60	+72	+38	+35	+22	+15	+12	0	−10	−8
A0.07	+10	+18	+25	+22	+20	+18	+15	+12	+16	+14	+5	−2
A1.01	0	+5	+10	+8	+5	+2	0	−2	−5	−8	−5	−12
A1.02	+8	+10	+15	+12	+10	+8	+5	+2	0	−2	+2	−5
A1.03	+5	+8	+12	+10	+8	+5	+2	0	−2	−5	−2	−10
A1.04	−2	0	+5	+2	0	−2	−5	−8	−10	−12	−8	−15
A1.05	+15	+18	+22	+20	+20	+18	+15	+12	+10	+8	+10	+2
A2.01	+25	+30	+35	+32	+32	+30	+28	+25	+20	+18	+20	+12
A2.02	+22	+25	+32	+30	+30	+28	+25	+22	+18	+15	+15	+8
A2.03	+28	+32	+38	+35	+35	+32	+30	+28	+22	+20	+22	+15
A2.04	−2	+2	+8	+5	+5	+2	0	−2	−5	−8	−8	−15
A2.05	+5	+10	+15	+12	+15	+12	+10	+8	+5	+2	−2	−10
(b) Building B												
B1.01	+0	+5	+12	+10	+15	+12	+8	+5	−2	−5	−8	−15
B1.02	+5	+10	+18	+15	+22	+18	+15	+10	+5	+2	−2	−10
B1.03	+2	+8	+15	+12	+18	+15	+12	+8	+2	0	−5	−12
B1.04	+8	+12	+20	+18	+25	+22	+18	+12	+8	+5	0	−8
B1.05	+2	+8	+15	+12	+18	+15	+12	+8	+2	0	−5	−12
B1.06	−2	+2	+8	+5	+10	+8	−8	−20	−44	−75	+2	+25
B1.07	+5	+12	+18	+15	+22	+20	+15	+12	+5	+2	−2	−8
B1.08	+2	+8	+15	+12	+18	+15	+12	+8	+2	−2	−5	−10
B1.09	+5	+10	+15	+12	+20	+18	+15	+10	+5	0	−2	−8
B1.10	+8	+15	+22	+20	+25	+22	+18	−8	+5	+2	−9	−5
B2.01	+12	+18	+25	+22	+25	+22	18	15	8	5	5	−2
B2.02	+18	+22	+30	+28	+32	+28	25	20	12	−2	−13	−20
B2.03	+10	+15	+22	+20	+28	+25	22	18	10	5	2	−5
B2.04	+15	+20	+38	+45	+50	+68	25	20	12	8	−2	0
B2.05	+12	+18	+25	+22	+25	+22	18	15	−1	0	5	−2
B2.06	+12	+15	+25	+22	+25	+7	−12	−15	0	5	−5	2
B2.07	+18	+20	+32	+28	+32	+28	25	−10	2	8	−18	4
B2.08	+15	+18	+28	+25	+28	+25	22	18	10	5	8	15

(Continues)

TABLE 8 | (CONTINUED)

	Sep	Oct	Nov	Dec	Jan	Feb	Mar	Apr	May	Jun	Jul	Aug
B2.09	+18	+20	+30	+48	+52	+72	25	20	12	8	−10	−12
B2.10	+15	+20	+28	+25	+30	+28	−5	10	−8	12	−2	0
B2.11	+20	+25	+35	+32	+38	+35	30	25	18	12	12	5
B2.12	+18	+22	+30	+28	+35	+32	28	22	15	10	10	2
						(c) Building C						
C0.01	+15	+20	+25	+22	+25	+22	+18	+12	+8	+5	−8	−12
C0.02	+22	+25	+30	+28	+32	+28	+25	+18	+12	+8	−2	−8
C0.03	+15	+18	+22	+20	+22	+20	+18	+12	+5	+2	−10	−12
C0.04	+20	+22	+28	+25	+30	+25	+22	+15	+10	+5	−5	−10
C1.01	−2	+2	+8	+5	+8	+5	−2	−5	−8	−15	−18	−66
C1.02	+5	+8	+12	+10	+15	+12	+8	+5	+2	−2	−8	−12
C1.03	+2	+5	+10	+8	+10	+8	+5	0	−2	−5	−12	−15
C1.04	+5	+8	+12	+10	+18	+15	+12	+8	+5	0	−10	−13
C1.05	+5	+8	+12	+10	+15	+12	+10	+5	+2	−2	−10	−15
C1.06	0	+5	+10	+8	+10	+8	+5	0	−2	−5	−15	−18
C1.07	+8	+12	+15	+12	+18	+25	+32	+52	+67	+2	−8	−12
C1.08	+5	+8	+12	+10	+2	−2	−10	−15	−28	−32	−15	−5
C1.09	+5	+10	+15	+12	+38	+45	+52	+78	+5	0	−8	−12
C2.01	+12	+15	+18	+15	+20	+18	+15	+10	+5	+2	−5	−8
C2.02	+18	+20	+22	+20	+25	+22	+20	−15	−3	+8	0	−2
C2.03	+10	+12	+15	+12	+18	+8	+2	0	−8	−10	+2	−6
C2.04	+15	+18	+20	+18	+12	+8	+5	−2	−5	+9	−2	−16
C2.05	+12	+15	+20	+18	+12	+8	+5	−2	−5	−15	−12	+3
C2.06	+8	+12	+18	+12	+8	+2	0	−8	−10	+1	−11	−23
C2.07	+15	+20	+25	+22	+28	+25	+71	+18	+12	−2	−18	−32
C2.08	+12	+15	+20	+18	+22	+18	+5	+2	−5	−8	−17	+2
C2.09	+15	+18	+22	+20	+25	+8	+5	−2	−5	+7	−12	−4
C2.10	+12	+15	+20	+18	+22	+20	+18	+12	−2	+5	−5	−8
C2.11	+18	+20	+25	+22	+48	+55	+32	+18	+2	−4	+7	−9
C2.12	+10	+12	+18	+15	+20	+18	+15	+10	+5	+2	−8	−10
C2.13	+15	+18	+22	+20	+25	+22	+20	+15	+10	+8	−2	−5
C2.14	+12	+15	+20	+18	+22	+20	+18	+12	+8	+5	−5	−8
C2.15	+18	+20	+25	+22	+28	+75	+22	+18	+2	−23	−18	−6
C2.16	+10	+12	+18	+15	+20	+18	+5	+2	−8	−10	−17	−33
C2.17	+15	+18	+22	+20	+10	+8	−2	−5	+10	+1	−7	−25
C2.18	+18	+20	+25	+22	+28	+25	+22	0	−5	+10	−18	−2

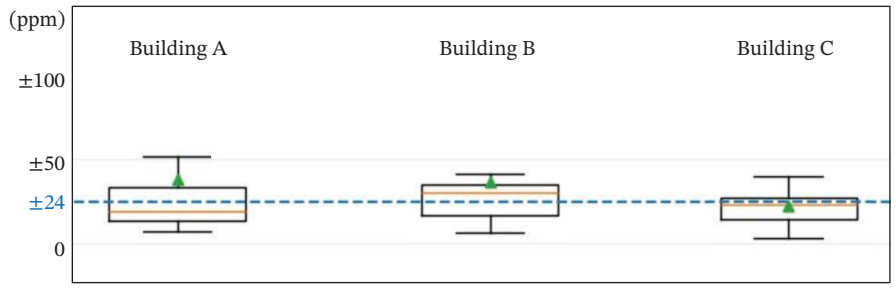

FIGURE 7 | Building drift rates relative to the CO_2 baseline.

- Monitor data during the first semester: September, October, November, December, and January.
- Tag CO_2 measurements according to three categories of monitored days/hours:
  - School days with working hours: This category includes days with scheduled academic activity within the opening and closing times (from 8 to 21 h) of the buildings. CO_2 measurements in this category correspond to periods when spaces may be occupied.
  - School days without working hours: This category refers to periods within school days when buildings are closed (from 21 to 08 h). These measurements are useful to understand how CO_2 levels drop to their minimum baseline values (ideally around 420 ppm) and rise again when activity resumes.
  - Nonworking days: This category includes Saturdays, Sundays, and holidays. CO_2 measurements during these days are useful for characterizing how minimum CO_2 levels stabilize over weekends or holiday periods and serve as a calibration reference.

From these premises, this paper proposes the following classification procedure (see Figure 8):

1. Define the time percentage when CO_2 >1500 ppm, and calculate it on school days with working hours:

$$T = \frac{\text{timestamps when } CO_2 > 1500 \text{ ppm}}{\text{total timestamps on school days with working hours}} \quad (1)$$

Define the monthly time percentage as time percentage (T) for each month from September to January.

$$T_M = \frac{\text{timestamps (in a month) when } CO_2 > 1500 \text{ ppm}}{\text{total timestamps (in a month) on school days with working hours}} \quad (2)$$

As Introduction describes, reducing T ensures that IAQ levels comply with health recommendations [6–9]. Figure 8 shows the T_M values between 0%–10% on the vertical axis. The horizontal axis lists all monitored spaces (A0.01–C2.19), organized in five columns for each month (left to right): September (black), October (orange), November (brown), December (red), and January (purple).

2. Observe and identify heterogeneity to propose an effective classification range for the case study: This approach can then be extrapolated to the range that best fits each context.
3. Select thresholds that allow the grouping of all spaces into R ranges: In this case study, $R = 5$ (A to E, see Table 9). Figure 8 highlights (with horizontal dashed lines) these five ranges: $T_M < 1\%$ (Range A), $T_M \in [1\% - 3\%]$ (Range B), $T_M \in [3\% - 5\%]$ (Range C), $TM \in [5\% - 7\%]$ (Range D), and $T_M > 7\%$ (Range E).
4. Assign each space to the range where its T_M value is highest, following a descending-discard criterion:

- If any T_M value exceeds 7%, the space is assigned to Range E; otherwise
- If any $T_M$value exceeds 5%, the space is assigned to Range D, and so on until Range A.
- For example: A2.01 (and A2.02, A2.03, A2.04, and A2.05), all showing $T_M > 7\%$, are ranged as E. A0.03 (and A1.01 and A1.02), which exceed 5% but not 7%, are ranged as D. Following this criterion, Figure 8 shades each space according to its range: pink (E), orange (D), blue (C), green (B), and yellow (A). Table 9 shows the monitored spaces classified for each of the five ranges.

5. Select the worst case space within each range (for each building): The worst-case means the space with the highest T_M value within each range. Figure 8 and Table 9 highlight in bold these worst-cases

For example: A2.01 (and A2.02, A2.03, A2.04, and A2.05), all showing $T_M > 7\%$, are ranged as E. A0.03 (and A1.01 and A1.02), which exceed 5% but not 7%, are ranged as D. Following this criterion, Figure 8 shades each space according to its range: pink (E), orange (D), blue (C), green (B), and yellow (A). Table 9 shows the monitored spaces classified for each of the five ranges.

5. Select the worst case space within each range (for each building): The worst-case means the space with the highest T_M value within each range. Figure 8 and Table 9 highlight in bold these worst-cases

This classification procedure provides a systematic way to organize the monitoring map and also helps interpret the context-award patterns revealed in Figure 8 However, for extrapolating this procedure to other tertiary buildings and scientific studies, it is necessary to confirm its statistical rigor. For this, we propose the following sensitivity analysis through two approaches. The first approach examines whether each space maintains (or not) its classification within its range when

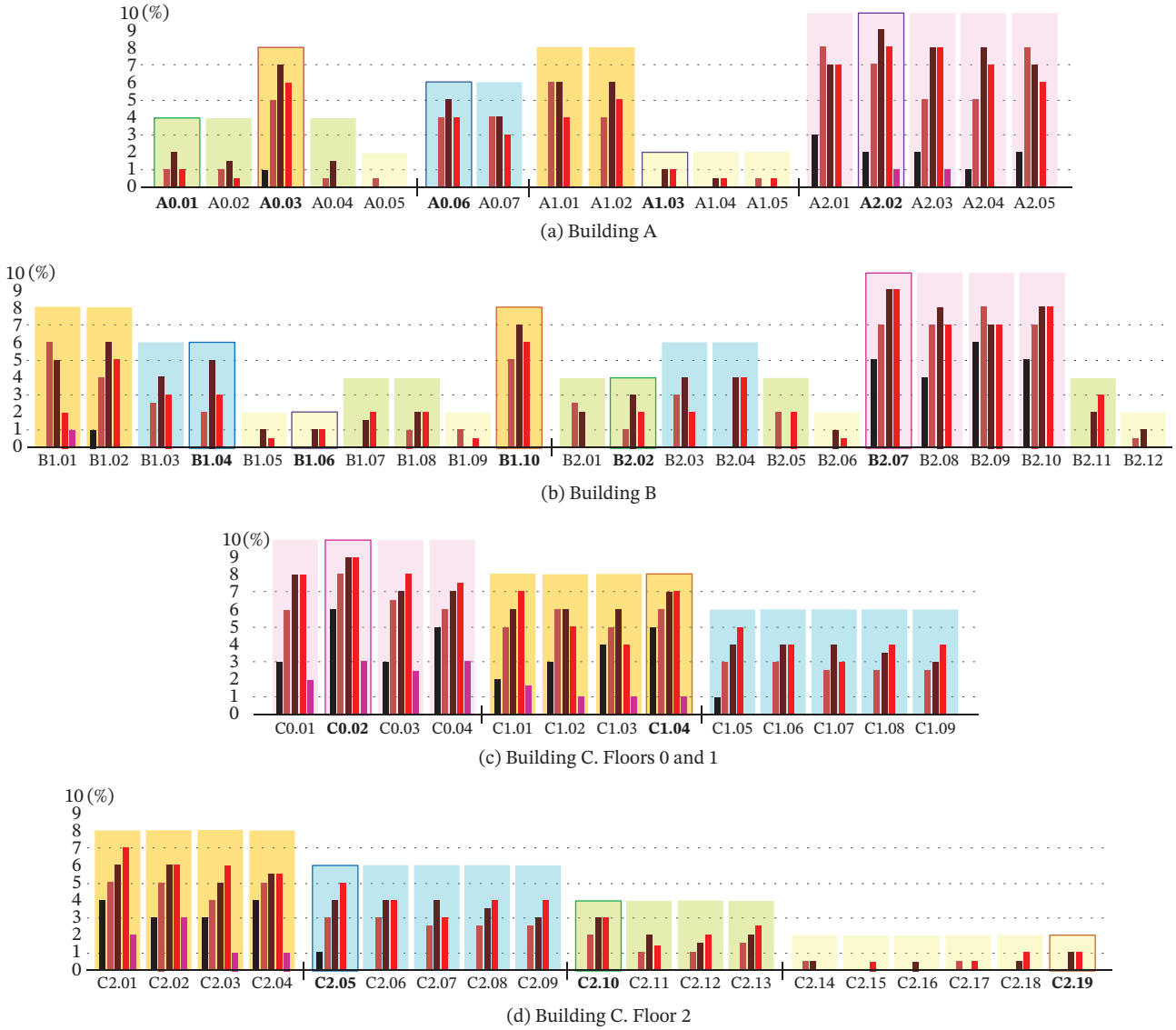

FIGURE 8 | Monitoring map: Monitored spaces colored by range and highlighted (in bold and remarked) the highest T_M percentages within each range. *Note:* Point 5 of the classification procedure indicates "Select the worst case space within each range (for each building). The worst case means the space with the highest T_M value within each range. Figure 8 and Table 9 highlight in bold these worst cases." The significance of bolded data in Figure 8 is the worst case within each range.

thresholds vary by ±10%. This provides an indicator of the robustness and well-scalability of the classification scheme. Beyond threshold variations, the second approach examines how quickly the classification converges over the months and identifies whether early classifications are representative or subject to further revision across the full year.

As a first approach, we have recalculated the space assignment with new ±10% thresholds. Thus, the new −10% thresholds are $T_M < 0.9\%$ (Range A), $T_M \in [0.9\% - 2.7\%]$ (Range B), $T_M \in [2.7\% - 4.5\%]$ (Range C), $T_M \in [4.5\% - 6.3\%]$ (Range D), $T_M > 6.3\%$ (Range E). And new +10% thresholds are: $T_M < 1.1\%$ (Range A), $T_M \in [1.1\% - 3.3\%]$ (Range B), $T_M \in [3.3\% - 5.5\%]$ (Range C), $T_M \in [5.5\% - 7.7\%]$ (Range D), and $T_M > 7.7\%$ (Range E). From the previously described T and T_M, we define the maximum of T_M in a study period (e.g., a semester or a full year).

$$T_{\mathrm{Mmax}} = \max_{(\mathrm{TM})} \tag{3}$$

After recalculating T_M and T_{Mmax} for new ±10% thresholds, Figure 9 highlights the spaces that change in range (shaded in blue). Of the 71 analyzed spaces, 9 spaces (12%) change their range when thresholds decrease by 10%, and only 1 space when thresholds increase by 10%. This means that 88%–99% of spaces retain their original classification under threshold variations. Furthermore, range changes are distributed across different buildings (two in Building A, three in Building B, and five in Building C), suggesting that sensitivity effects are space-specific and not driven by building-level bias. Such behavior is indicative of a stable and well-scaled classification scheme where ranges are not excessively sensitive to changes in thresholds. Moreover, all changes involve transitions between adjacent ranges (from B to C, C to D, and D to E or E

TABLE 9 | Monitored spaces classified by range and highlighted (in bold) the highest T_M percentages within each range.

Range	$CO_2 > 1500$	Building A	Building B	Building C
A	**<1%**	A0.05,	B1.05,	C2.14,
			B1.06,	C2.15,
			B1.09,	C2.16,
		A1.03,	B2.06,	C2.17,
		A1.04,	B2.12	C2.18,
		A1.05		**C2.19**
B	**1%–3%**	**A0.01**,	B1.07,	**C2.10,**
		A0.02,	B1.08,	C2.11,
		A0.04	B2.01,	C2.12,
			B2.02,	C2.13
			B2.05,	
			B2.11	
C	**3%–5%**	**A0.06**,	B1.03,	C1.05,
		A0.07	**B1.04**,	C1.06,
				C1.07,
				C1.08,
				C1.09,
			B2.03,	**C2.05**,
			B2.04	C2.06,
				C2.07,
				C2.08,
				C2.09
D	**5%–7%**	**A0.03**,	B1.01,	C1.01,
		A1.01,	B1.02,	C1.02,
		A1.02	**B1.10**	C1.03,
				C1.04,
				C2.01,
				C2.02,
				C2.03,
				C2.04
E	**>7%**	A2.01,	**B2.07,**	C0.01,
		A2.02,	B2.08,	**C0.02**,
		A2.03,	B2.09,	C0.03,
		A2.04,	B2.10	C0.04
		A2.05		

Note: Point 5 of the classification procedure indicates "Select the worst case space within each range (for each building). The worst case means the space with the highest T_M value within each range. Figure 8 and Table 9 highlight in bold these worst cases". The significance of bolded data in Table 9 is the worst case within each range.

to D), without jumping across ranges. This behavior confirms that classification boundaries are coherently ordered without range discontinuities.

As a second approach, we determine the time window necessary to ensure the stability and convergence of the procedure. For this, the classification is recomputed using progressively longer windows (W_i): W_1 with the first month only, W_2 with the first 2 months, W_3 with the first 3 months, and so on with i from 1 to 5. We define:

$$TW_i = \frac{\text{timestamps (in the first i – months) when } CO_2 > 1500 \text{ ppm}}{\text{total timestamps (in the first i – months) on school days with working hours}} \quad (4)$$

$$T_{\text{Wi max}} = \max\left(T_{\text{Wi}}\right) \quad (5)$$

Thus, after recalculating T_{Wi} and $T_{\text{Wi max}}$ (for W_1 to W_5 in the study period of 5 months) out of the 71 analyzed spaces: 13 spaces converge in W_1 (after the first month), 17 in W_2, 37 in W_3, and only 4 spaces require 4 months to stabilize. This means that +94% of spaces converge within the first 3 months. This convergence analysis shows that the proposed classification procedure captures structural CO_2 patterns rather than transient effects: three monitored months are sufficient to obtain a stable categorization.

After statistically ensuring the validity and replicability of the classification procedure, Table 10 summarizes the selected spaces, detailing their key contextual factors: orientation (N = north, S = south, E = east, W = west), location (building = A / B / C and floor = 0 / 1 / 2), size (large, medium, and small), and occupancy (high, moderate, low).

Before moving into the IAQ study detailed in the next section, the key insights highlighted with this monitoring map are useful to translate into actionable interventions for new deployments in three stages:

- A priori decisions: Monitoring map shows substantial differences between spaces that a priori may appear similar according to architectural plans. For example, A0.03, A0.04, and A0.05 (similar in size and located on the same floor, as shown in Figure 5) are classified into different ranges (D, B, and A, respectively). As analyzed in the next section, this divergence is explained by key factors such as orientation, location, size, occupancy, and scheduling. As discussed in Conclusions, this can be translated into an intervention tool through a predictive sorter using a neural-network weight-vector algorithm. Furthermore, this monitoring map justifies the $n \ll N$ strategy with statistical significance. Once all the potentially locations (N) can be grouped into a set of representative spaces (n), the IAQ study can be sustainable and cost-effective
- Comprehensive view: This map provides a large-scale overview of the IAQ levels throughout time and space. It shows how CO_2 behavior significantly varies across several months within the same space. This is attributed to the changing rhythms of university activities throughout the semester: September (black) and January (purple) show the lowest attendance due to (respectively): start of the academic period (without practical sessions or coursework), and the exam period (without classes). October (orange), November (brown), and December (red) show higher attendance, resulting in higher CO_2 percentages. By revealing this variability, classification provides a structured way to interpret IAQ behavior in relation to underlying contextual factors such as schedules, usage patterns, and seasonal fluctuations.
- Long-term strategies: The set of representative spaces selected from this monitoring map can follow a rotation schedule. Once the classification procedure groups all the spaces in R ranges, the CO_2 monitors can be moved to other spaces of the same range each season (autumn–winter vs.

Space	Previous		T_{Mmax}	-10% threshold		+10% threshold	
	T_M interval	Range		T_M interval	Range	T_M interval	Range
A0.03	5% – 7%	D	6.8	> 6.3%	E	5.5 – 7.7%	D
A0.06	3% – 5%	C	4.7	4.5 – 6.3%	D	3.3 – 5.5%	C
B1.04	3% – 5%	C	4.8	4.5 – 6.3%	D	3.3 – 5.5%	C
B1.10	5% – 7%	D	6.9	> 6.3%	E	5.5 – 7.7%	D
B2.02	1% – 3%	B	2.9	2.7 – 4.5%	C	1.1 – 3.3%	B
C1.04	5% – 7%	D	6.9	> 6.3%	E	5.5 – 7.7%	D
C1.05	3% – 5%	C	4.7	4.5 – 6.3%	D	3.3 – 5.5%	C
C2.01	5% – 7%	D	6.8	> 6.3%	E	5.5 – 7.7%	D
C2.05	3% – 5%	C	4.9	4.5 – 6.3%	D	3.3 – 5.5%	C
C0.04	> 7%	E	7.4	> 6.3%	E	5.5 – 7.7%	D

FIGURE 9 | Monitored spaces that change in range with the new ± 10% thresholds.

TABLE 10 | Selected spaces for the IAQ study.

		Location		Size			Occupancy		
Selected space	**Orientation**	**Building**	**Floor**	**Large**	**Medium**	**Small**	**High**	**Moderate**	**Low**
A1.03	E	A	1		•				•
A0.01	E	A	0		•			•	
A0.03	E	A	0		•		•		
A0.06	S	A	0	•			•		
A2.02	E	A	2			•	•		
B1.06	S	B	1	•					•
B2.02	S	B	2	•				•	
B1.10	N	B	1	•			•		
B1.04	S	B	1		•			•	
B2.07	N	B	2			•	•		
C2.19	S	C	2			•			•
C2.10	S	C	2		•			•	
C2.05	N	C	2		•			•	
C1.04	N	C	1	•			•		
C0.02	N	C	0	•			•		
Canteen	W	A	0	•			•	•	•
Canteen	N	C	0	•			•	•	•
Library	W	C	1	•			•	•	•

spring–summer) or each academic course. This strategy supports the CO_2-based ventilation assessment system and reinforce the sensitivity analysis of the proposed descending-discard criterion. Furthermore, because the proposed selection, placement and calibration procedures follow criteria of portability, autonomy, and connectivity, the reconfiguration of these IoT-driven solutions remains their cost-effective feature.

3.2 | IAQ Study

Building on the previous classification procedure, this section analyzes the IAQ behavior of each selected space in the three buildings. As World Health Organization (WHO) suggests [4], IAQ is determined by air pollutants, such as volatile organic compounds (VOC), formaldehyde and particulate matters (PM) (specifically PM2.5 and PM10), among other biological and chemical factors. As the first step of the proposed IAQ study, this paper considers the maximum allowable values for these pollutant concentrations:

- Formaldehyde is often present in buildings indoors, mainly originating from chipboard and other materials derived from wood, equipment, treatments, hygiene and cosmetic products, and exhaust gases. Several international organizations regulate their recommended thresholds for daily exposure. WHO guideline [11] sets a limit value of 100 parts

per billion (ppb) or 100 $\mu g/m^3$. In Spain, Directive UNE-EN 16798-1:2020 [6] sets four thresholds for indoor formaldehyde concentrations: not significant (< 20 $\mu g/m^3$), weakly significant (20–50 $\mu g/m^3$), strongly significant (50–100 $\mu g/m^3$), and extremely significant (> 100 $\mu g/m^3$).

- PMs are suspended particles often because of inadequate air ventilation. Their presence in buildings indoors can harmfully impact eye irritation, headaches, fatigue, and even respiratory diseases (e.g., allergies and asthma). The Environmental Protection Agency (EPA) and National Ambient Air Quality Standard (NAAQS) [12] set maximum daily average of 35 $\mu g/m^3$ (for PM2.5) and 150 $\mu g/m^3$ (for PM10). Directive 2008/50/EC [7] sets daily averages of 20 $\mu g/m^3$ (for PM2.5) and 45 $\mu g/m^3$ (for PM10), and WHO air pollution guidelines [13] decrease these daily averages to 15 $\mu g/m^3$ (for PM2.5) and 40 $\mu g/m^3$ (for PM10).

From these considerations, Figure 10 shows the obtained real measurements (in $\mu g/m^3$, see vertical axis) represented with their maximum (red), average (blue), and minimum (green) daily values for each selected space (see horizontal axis) within the monitored months (September to January) when the space is occupied. In Figure 10a, formaldehyde shows low values (between 1 and 14 $\mu g/m^3$), well below the maximum limit established by the recommended thresholds (marked by yellow horizontal lines). For PM, the values range between 2 and 9 $\mu g/m^3$ (see Figure 10b for PM2.5), and between 1 and 9 $\mu g/m^3$ (see Figure 10c for PM10). In all cases, these daily concentrations are well below the recommended thresholds (marked by yellow horizontal lines). This confirms that the international regulations are being followed in all spaces.

These results justify that subsequent study focuses on CO_2 as a key IAQ indicator and its interrelations with occupancy patterns, space size, architectural characteristics, and contextual factors. Thus, Figures 11, 12, 13, 14, 15, 16, 17, 18, 19, 20 and 21 continue the IAQ study by illustrating the CO_2 real measurements in each selected space. In these figures, the vertical axis represents the monitored months (September to January), whereas the horizontal axis represents the percentage of time (from 50% to 100%) during school days with working hours in which the monitored CO_2 concentration fulfills the international recommendations [6–9]: CO_2 level < 800 ppm (dark green), 800–1000 ppm (light green), 1000–1500 ppm (orange), and > 1500 ppm (red).

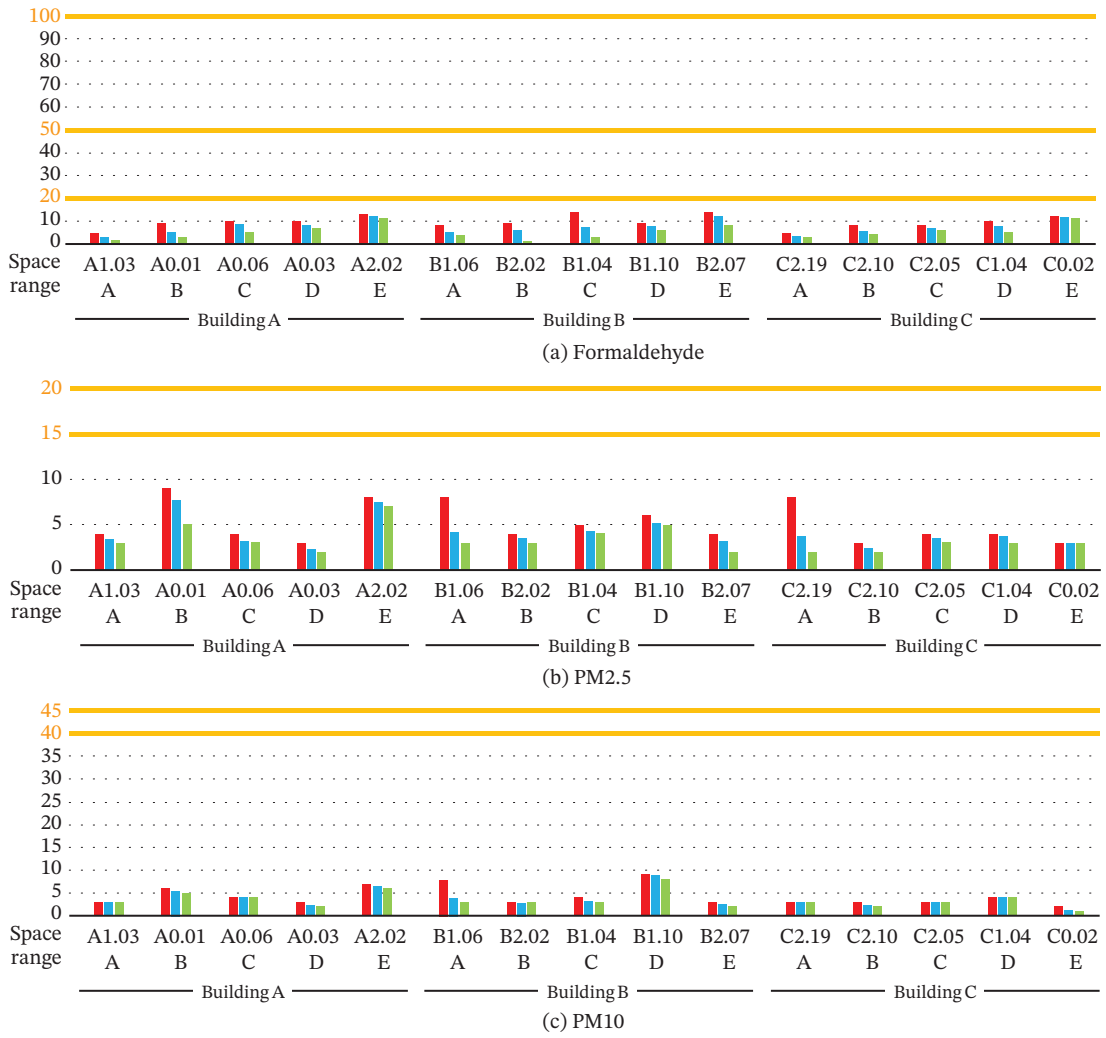

FIGURE 10 | Air pollutants.

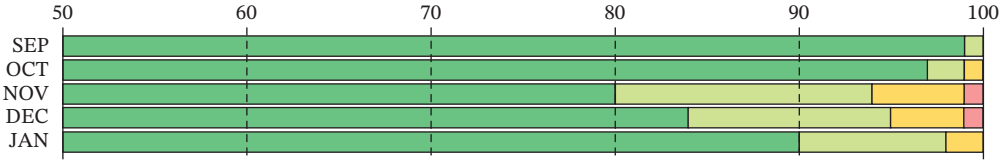

FIGURE 11 | Building A: Range A—low occupancy (A1.03).

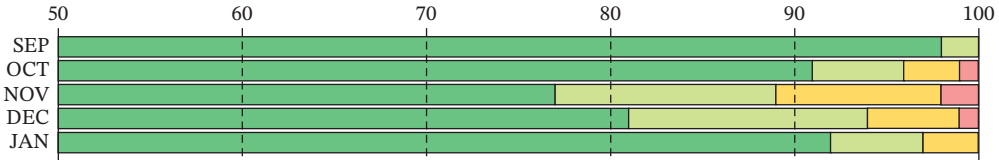

FIGURE 12 | Building A: Range B—moderate occupancy (A0.01).

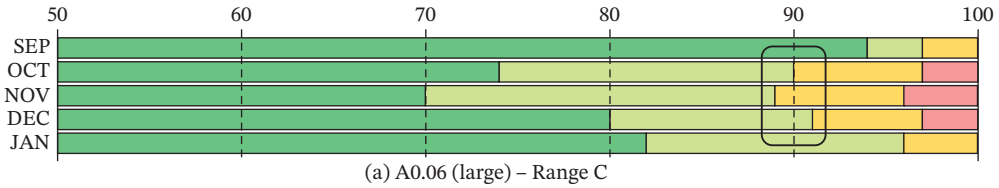

(a) A0.06 (large) – Range C

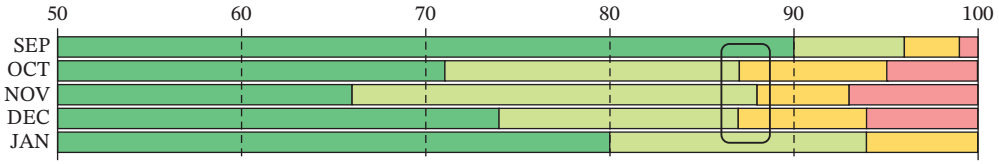

(b) A0.03 (medium) – Range D

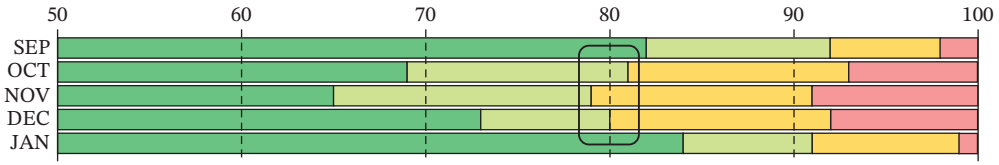

(c) A2.02 (small) – Range E

FIGURE 13 | Building A: high occupancy.

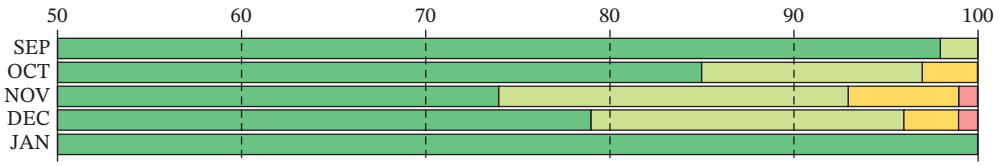

(a) B1.06 (low occupancy) – Range A

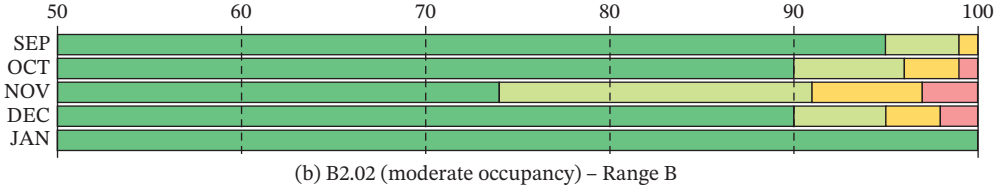

(b) B2.02 (moderate occupancy) – Range B

FIGURE 14 | Building B: large size.

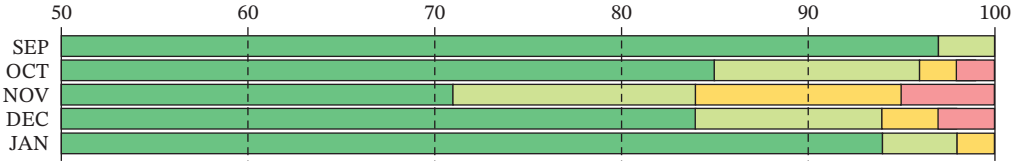

FIGURE 15 | Building B: medium size and moderate occupancy (B1.04)—Range C.

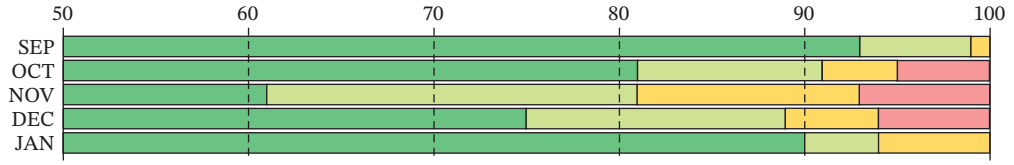

FIGURE 16 | Building B: large size and high occupancy (B1.10)—Range D.

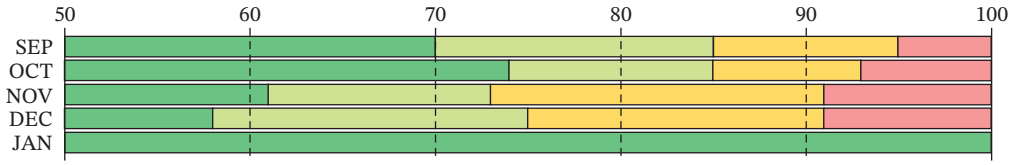

FIGURE 17 | Building B: Small size and high occupancy (B2.07)—Range E.

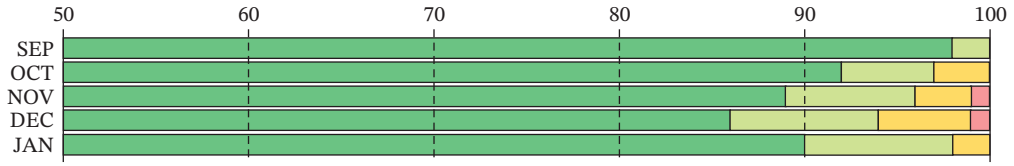

FIGURE 18 | Building C: small size and low occupancy (C2.19)—Range A.

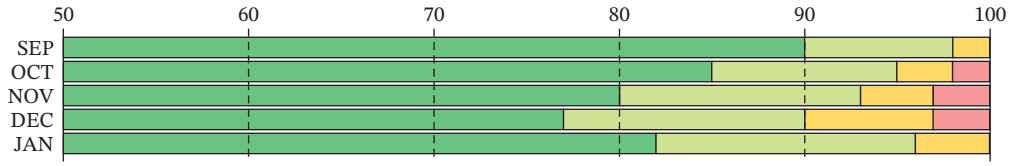

(a) South orientation (C2.10) – Range B

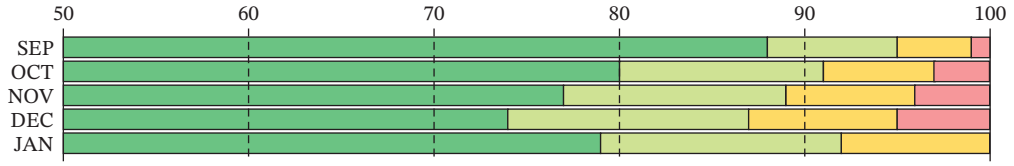

(b) North orientation (C2.05) – Range C

FIGURE 19 | Building C: medium size with moderate occupancy.

3.2.1 | Building A

The analysis begins with Building A, examining representative spaces according to occupancy, from the lowest CO_2 levels (A1.03, low occupancy; A0.01, moderate occupancy) to the highest CO_2 levels with high occupancy (A0.06, large; A0.03, medium; A2.02, small). Figure 11 shows the best IAQ conditions in A1.03 (low occupancy). All months show that the values of $CO_2 < 1000$ ppm for over 94% of the time: 99% in October, 94% in November, 95% in December, and 98% in January.

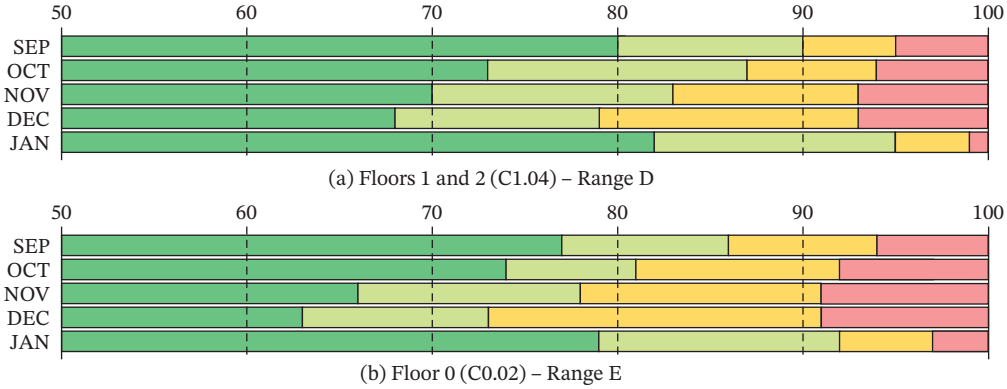

FIGURE 20 | Building C: large size with high occupancy.

FIGURE 21 | Variable occupancy

Figure 12 shows the results for A0.01 (moderate occupancy). IAQ levels are similar to those in A1.03, but owing to a higher occupancy, the percentage of time with $CO_2 > 1000$ ppm increases by approximately 1%–5% in all months (A0.01 vs. A1.03): 1% versus 4% (October), 6% versus 11% (November), 5% versus 6% (December) and 2% versus 3% (January). These results confirm that higher occupancy directly increases CO_2 concentrations.

To confirm the relationship between occupancy and CO_2, Figure 13 compares three high-occupancy spaces of different sizes: A0.06 (large), A0.03 (medium) and A2.02 (small). The highest CO_2 levels consistently occur in the smallest space. A first observation is that the time percentage in lower CO_2 categories decreases as size decreases. $CO_2 < 1000$ ppm shows this size-dependent progression: 97% > 96% > 92% (September), 90% > 87% > 81% (October), 89% > 88% > 79% (November), 91% > 87% > 80% (December), and 96% > 94% > 91% (January). This indicates that smaller spaces reach higher CO_2 levels more quickly when densely occupied.

A second observation concerns environmental health performance. As size decreases, IAQ conditions worsen, reflecting a progressive increase in $CO_2 > 1500$ ppm during the busiest months (periods of highest teaching activity and therefore highest occupancy): 3% < 5% < 7% (October), 4% < 7% < 9% (November), and 3% < 6% < 8% (December). These results ensure acceptable IAQ levels: $CO_2 > 1500$ ppm always remains below 9%; moreover, $CO_2 < 1000$ ppm remains for approximately 90% of the time in large spaces, 87% in medium spaces, and 80% in small spaces.

3.2.2 | Building B

To validate the trends observed in Building A, the IAQ study continues with building B by analyzing the size–occupancy ratio. Figure 14 shows results obtained for the largest spaces (B1.06 and B2.02). Both maintain very good IAQ levels: $CO_2 < 1000$ ppm for over 95% of the time (slightly lower, ~90%, in November). B1.06 (low occupancy) consistently outperforms B2.02 (moderate occupancy) in terms of $CO_2 < 1000$ ppm: October (97% vs. 96%), November (93% vs. 91%), and December (96% vs. 95%); including B2.02 also shows a higher occurrence of $CO_2 > 1500$ ppm (1% in October, 3% in November, and 2% in December). Figures 16 and 17 reinforce these trends, which

become more pronounced depending on the specific size–occupancy combination. Thus, B1.04 (medium size and moderate occupancy) shows better IAQ than B1.10 (large size and high occupancy) for $CO_2 < 1000$ ppm between 3% and 5%: 96% versus 91% (October), 84% versus 81% (November), 94% versus 89% (December), and 98% versus 94% (January). These improvements are even clearer for $CO_2 < 800$ ppm between 4% and 10%: 85% versus 81% (October), 71% versus 61% (November), 84% versus 75% (December), and 94% versus 90% (January). These trends intensify during months with more teaching activity and therefore higher occupancy. Since Building B hosts first-year courses with high attendance, occupancy peaks in November (followed by October and December) translate into a triangular CO_2 pattern (in red).

These trends become even clearer when analyzing a small and high-occupancy computer lab (B2.07). As shown in Figure 17, except for January (with no practical sessions, $CO_2 < 800$ ppm 100% of time), this lab shows high CO_2 concentrations both $CO_2 > 1000$ ppm (15% in September and October, 27% in November, and 25% in December) and $CO_2 > 1500$ ppm (5% in September, 7% in October, and 9% in November and December). These data are ascribed to the specific usage characteristics of a computer lab: practical teamwork sessions and collaborative tasks, with interactions (talking, moving, and sharing resources) between students and teachers, which continuously produces exhaled air that increases CO_2 concentration.

3.2.3 | Building C

The IAQ study concludes with Building C, performing an analysis according to size, from small (with low occupancy) to medium (with moderate occupancy) and large (with high occupancy). Beginning with small-size spaces (C2.14–C2.19), without fixed schedule (they require prior reservation), implying low and variable occupancy. As shown in Figure 18, this feature yields very good IAQ levels with $CO_2 < 1000$ ppm above 94% of the time. CO_2 levels slightly rise above 1000 ppm in months with more teaching activity: 3% (October), 4% (November), 6% (December), and 2% (January).

Following with medium-size spaces (and moderate occupancy), orientation and weather become relevant. Figure 19 compares C2.10 (south-facing) and C2.05 (north-facing). In both cases $CO_2 > 1000$ ppm progressively increases as outdoor temperatures decrease from September to December. IAQ levels improve in January ($CO_2 < 1000$ ppm above 90% of the time) owing to Christmas holidays and exam periods, when occupancy becomes more variable. Figure 19 also shows how $CO_2 > 1000$ ppm worsens between 3% and 4% in north-facing versus south-facing spaces: 5% versus 2% (September), 9% versus 5% (October), 11% versus 7% (November), and 13% versus 10% (December). This trend is understandable because south-facing spaces have higher solar gains, which lead to the opening of windows, thus reducing CO_2 levels. Windows typically remain closed in north-facing spaces to preserve thermal comfort, increasing $CO_2 > 1500$ ppm between 1% and 2% comparing C2.05 versus C2.10: 1% versus 0% (September), 3% versus 2% (October), 4% versus 3% (November), and 5% versus 3% (December).

Figure 20 highlights similar trends in large-size spaces (with high-occupancy). Again, $CO_2 > 1000$ ppm progressively increases from September to December due to colder weather and the temperature drop. Furthermore, the comparison among floors shows a clear gradient. Figure 20 highlights how Floor 0 (colder than Floors 1 and 2) shows higher CO_2 levels because windows remain closed more often. Comparing C1.04 (Floors 1 and 2) versus C0.02 (Floor 0) $CO_2 > 1000$ ppm decreases between 4% and 6%: 14% versus 10% (September), 19% versus 13% (October), 22% versus 17% (November), and 27% versus 21% (December).

To complete the IAQ study, we examine variable-occupancy spaces. Figure 21a,b shows the campus canteens, which are both large and generally well-ventilated. Although briefly crowded during meal hours (14–15 h), average $CO_2 > 1000$ ppm remains below 10%. This demonstrates that, under variable occupancy, the size factor does not significantly influence IAQ. Comparing the medium-size canteen (Building A) with the large-size one (Building C), $CO_2 > 1000$ ppm decreases by 3%: 6% versus 3% (November), 9% versus 6% (December), and 10% versus 7% (January). Figure 21c shows the campus library, a large and well-ventilated space with inherently low CO_2 levels because occupants are mostly studying quietly with minimal exhaled CO_2. In September and October, as students have not yet fully occupied the library, $CO_2 < 800$ ppm remains 100% of the time. As occupancy increases during the exam periods, $CO_2 > 1000$ ppm rises proportionally: 3% (November), 6% (December), and 7% (January). Nonetheless, all the measurements comply with IAQ norms.

Finally, to support all these experimental results with formal hypothesis testing, this paper includes two nonparametric analyses: Mann–Whitney U test, for two-sided pairwise comparisons; and Kruskal–Wallis test, for comparisons involving more than two spaces. Table 11 shows the p value of these tests over all the CO_2 study (Figures 11, 12, 13, 14, 15, 16, 17, 18, 19, 20, and 21), focusing on the critical CO_2 bands: 1000–1500 ppm (orange); and >1500 ppm (red). Across all the results, p values are nonsignificant: This means that data interpretation is statistically consistent within its CO_2 behavior. Only two p values (shaded in blue) are high: for >1500 ppm, in Figures 19 and 20, related to north–south orientation and comparison among floors. This may be attributed to the variability of human behavior, suggesting the interest for further characterization of the window opening and closing.

TABLE 11 | Statistic p value for each CO_2 analysis from Mann–Whitney U test and Kruskal–Wallis tests.

Figures	10	11	12	13	14	15	16	17	18	19	20
1000–1500	0.144	0.144	0.008	$4 \cdot 10^{-18}$	0.045	$6 \cdot 10^{-7}$	$6 \cdot 10^{-7}$	$2 \cdot 10^{-8}$	0.002	0.260	$3 \cdot 10^{-16}$
>1500	0.049	0.049	0.153	$9 \cdot 10^{-13}$	$3 \cdot 10^{-10}$	0.010	0.010	$1 \cdot 10^{-6}$	0.525	0.472	$4 \cdot 10^{-13}$

TABLE 12 | Intervention proposals from measurements obtained under real conditions.

Current operations	Data-driven strategies
For each degree or master programs, a same class group teaches all its subjects in the same classroom of a building	From enrollment data for each subject, assign the most suitable classroom (preferably in a same building) according to studied factors: orientation, location, and size
Natural ventilation is not programmed: window opening/closing depends on human behavior.	From north/south–facing spaces as regarding seasonal weather (as Building C shows), assign highest occupancy subjects to best orientation classroom with lowest CO_2 levels
IoT ecosystem collects CO_2 measurements in real-time but analysis is done every 6 months at the end of each seasonal semester (autumn–winter and spring–summer)	From real-time CO_2 measurements, perform a weekly analysis (as next section details). Use this day-pattern guide for CO_2-based ventilation for each day of next week

As summarized contribution from all these real measurements and trends, Table 12 advances several data-driven strategies as intervention proposal for new CO_2-based deployments. This constitutes several examples of decision-making under real conditions as preliminary step for automated algorithms and predictive models.

3.3 | Analysis of CO_2 Evolution

To complement the IAQ study, this section analyses CO_2 evolution, both day-by-day and hour-by-hour, to understand how CO_2 behaves in relation to the types of days, patterns of space use, ventilation strategies, and human behavior. Figure 22 shows day-by-day CO_2 evolution in a standard space (medium size and moderate occupancy) for 3 months (horizontal axis): November, December, and January. Each colored point represents the daily maximum CO_2 concentration ($CO_{2_{max}}$): green ($CO_{2_{max}} < 1000$ ppm), yellow (1000–1500 ppm), and red ($CO_{2_{max}} > 1500$ ppm). The goal of this representation is not to analyze daily values in detail, but rather to understand their evolution across weeks. Figure 22 provides the following insights:

- Weekend identification.: The last two points of every week are always green because the building is closed (Saturday and Sunday), and $CO_{2_{max}}$ remains below 1000 ppm. This has two interesting implications:
  - It confirms that minimum values correspond to the reference baseline of the CO_2 monitors (around 420 ppm): if these values do not correspond to their reference baseline, they would require calibration.
  - It marks the start and end of each week, helping interpret weekly IAQ cycles through CO_2 levels.

TABLE 13 | Class scheduling for the analyzed days.

	08–09	09–10	10–11	11–12	12–13	13–14	14–15	15–16	16–17	17–18	18–19	19–20	20–21
Day 1	Class	Class				Class		Class	Class	Class	Class		
Day 2	Class	Class				Reserved		Class	Class	Class	CLASS		
Day 3		Class	Class		Class	Class		Class	Class	Class			
Day 4		Class	Class				Class	Class					
Day 5						Reserved			Class	Class			

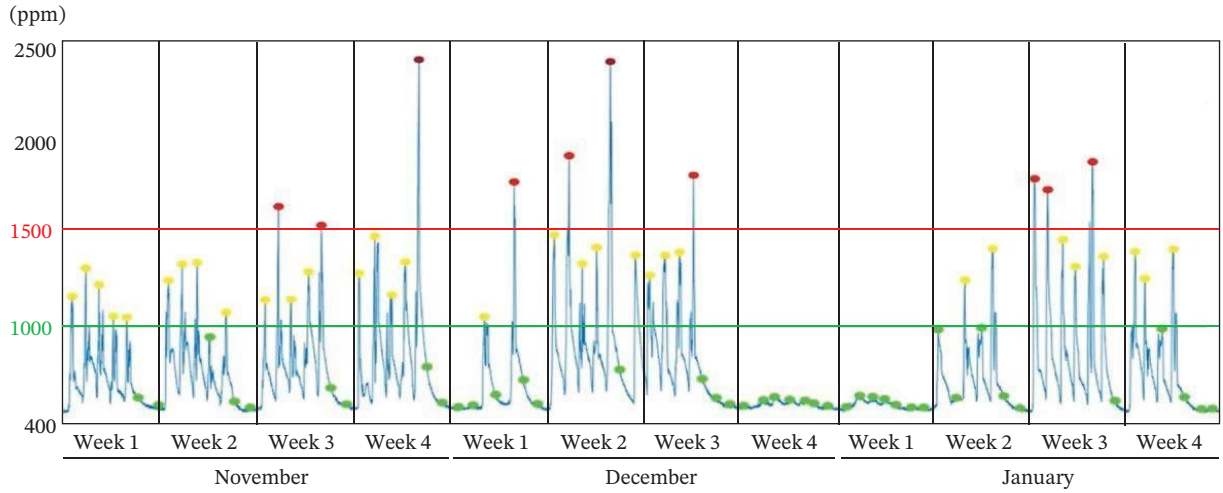

FIGURE 22 | Day-by-day CO_2 evolution.

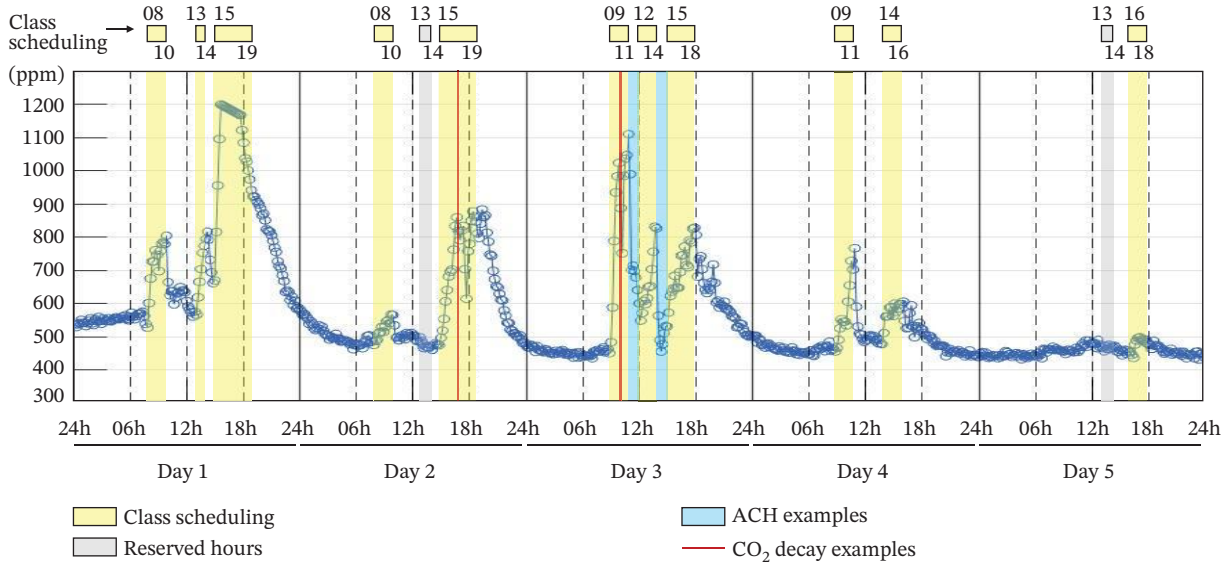

FIGURE 23 | Hour-by-hour CO_2 evolution.

- Detection of non-working days and holidays: Green points on nonweekend days indicate building closure:
  - December, Week 1 (Days 1, 2, and 4), corresponds to Spain's national holidays, namely Constitution Day (December 6) and the Immaculate Conception (December 8).
  - December (Week 4) and January (Week 1) correspond to the Christmas break.
  - These results suggest that IoT monitoring can detect unplanned presence or absence in closed buildings.
- General IAQ performance: Most $CO_{2_{max}}$ values remain below 1000 ppm (~70%) and 1500 ppm (~90%), with only occasional excursions (red dots). This provides a global view of IAQ performance and illustrates how IoT monitoring enables data-driven decisions by detecting critical high-CO_2 situations.

These day-by-day insights lead to move toward a detailed hour-by-hour analysis to understand how CO_2 evolves in relation to class scheduling, occupancy cycles, breaks between classes, natural ventilation events, and the variability of human behavior in these environments. For this, Table 13 summarizes a set of five school days, as representative class scheduling periods. Timeslots in yellow are morning and afternoon classes (with midday multipurpose periods), and timeslots in grey are reserved hours (for tutoring, teamwork, etc.). Figure 23 shows the hour-by-hour CO_2 evolution (ppm on the vertical axis) for these 5 days. The upper horizontal axis adds (in yellow) shows the class scheduling (with the start and end times), and the lower horizontal axis delimits each day, marked (with dotted lines) by 6-h intervals: 06, 12, 18, and 24 h.

Figure 21 highlights the following findings:

- Alignment between CO_2 evolution and class scheduling: Periods where CO_2 rises and falls (shaded in yellow) closely correspond to the start and end of classes. This further confirms the direct relationship between CO_2 concentration and occupancy. Additionally, CO_2 measurements show that reserved hours (shaded in grey) were not actually occupied (Days 2 and 5 between 13 and 14 h), demonstrating that CO_2 may be used to detect human behavioral variability.
- Air-change dynamics between class periods: The CO_2 evolution between classes indicates the air changes per hour (ACH) indicator. ACH is a quantitative measure of how many times per hour the air is replaced and, consequently, this guarantees the IAQ levels. Under well-mixed ventilation, the amount of air changed would be upper to: 60% after 1 ACH, 80% after 2 ACH, and 95% after 3 ACH. Monitored CO_2 follows these ACH patterns as two examples (shaded in blue) show:

- Day 3: CO_2 enhances from 1100 to 550 ppm between 11 and 12 h (around 80% reduction after 1 ACH).
- Day 3: CO_2 enhances from 850 to 450 ppm between 14 and 15 h (around 60% reduction after 1 ACH).
- CO2 decay during short breaks between consecutive classes also reflects ACH behavior (red vertical lines):
- Day 2: 850 to 600 ppm with 1 ACH at 17 h in the class change between 15–17 h and 17–19 h.
- Day 3: 1000 to 750 ppm with 1 ACH at 10 h in the intermediate class break between 09 and 11 h.

- CO_2 decay outside class hours. CO_2 evolution during longer unoccupied periods quantifies CO_2 decay rates, which tend toward baseline values (around 420 ppm). Figure 21 illustrates these decay patterns to baseline: from 1150 ppm in 12 h (Day 1), from 900 ppm in 6 h (Day 2), from 800 ppm in 9 h (Day 3), from 600 ppm in 5 h (Day 4), and from 500 ppm in 2 h (Day 5). These results show a nonlinear decay behavior, suggesting the interest for further quantitative characterization (e.g., logarithmic decay slope) as an initial step toward more detailed ACH modeling.

4 | Conclusions: Further Research

This paper presents a real-time monitoring IoT ecosystem for managing indoor CO_2 concentrations to improve IAQ conditions across a smart university campus. The results contribute to a CO_2 characterization that supports data-driven decision-making from real measurements. This methodological framework bridges the gap between simulated and real operating conditions, providing replicable procedures and a practical and context-aware approach suitable for heterogeneous educational buildings and extrapolated to tertiary buildings.

First contribution of this paper is a comprehensive methodology of systematic procedures for deploying a real-time IoT monitoring ecosystem. This methodology proposes three sequential stages for CO_2 monitors:

- Selection: This paper selects two CO_2 monitors (Milesight AM307 and Aranet4 Pro) by comparing their key criteria for portability, autonomy, and connectivity. This allows their relocation in new deployments.
- Placement: Following the criterion of highest CO_2 levels, this paper chooses the locations near the teaching area (P1 or P2) with an extrapolation procedure to other typologies based on space layout and key use areas.
- Calibration: With a criterion of 90% compliance, this paper sets calibration thresholds of +65 ppm (upper) and −55 ppm (lower). It also proposes a periodic check procedure based on minimum CO_2 values (reference baseline around 420 ppm) measured during nonworking hours (from 21 to 08 h) and nonworking days.

The challenges addressed in each stage enable to replicate this methodology in tertiary buildings to select, install, and calibrate CO_2 monitors. To guide practitioners in new deployments, these stages would be:

- Select the key features from criteria comparison (see Table 2) to choose the most suitable CO_2 monitors.
- Identify strategic placements (as P1 and P2) with potentially highest CO_2 levels to locate CO_2 monitors.
- Calibrate CO_2 monitors and check their measures during nonworking periods as recalibration procedure.

From this methodology, this paper proposes three types of approaches to support informed decision-making under real conditions: a campus-wide monitoring map, an IAQ study, and an analysis of CO_2 evolution. Firstly, this paper contributes with a monitoring map as classification procedure with three key points:

- A priori decisions: Beyond an architectural criterion, spaces can be classified by their contextual factors. The classification procedure groups spaces from their key features: orientation (north, south, east, and west), building (A, B, and C), floor (0, 1, and 2), size (large, medium, and small), and occupancy (high, moderate, and low). This procedure justifies the $n \ll N$ strategy with statistical significance. Once all potentially locations (N) can be grouped in a set of representative spaces (n), the IAQ study can be sustainable and cost-effective. In this work, with CO_2 monitors costing between €150 and €250 (see Table 2), reducing from $N = 71$ to $n = 15$ means an average saving of €12,000 along with more efficient seasonal maintenance, operational and upgrade costs.
- Comprehensive view: This map provides a large-scale initial overview of the IAQ levels across all spaces, verifying if CO_2 levels fulfill international recommendations and detecting potential critical situations. Therefore, this offers a method to explicitly integrate into the IAQ study their contextual factors (schedules, usage patterns, seasonal fluctuations,

etc.) and to subsequently advance toward cross-related analysis.

- Long-term strategies: The set of representative spaces can be replaced to other space of the same range each season or academic course. This enables sensitivity analyses of IAQ study remaining its cost-effectiveness.

From the monitoring map, the measurements from the IAQ study within the CO_2 evolution analysis provide two complementary approaches. The first relates to occupancy-driven factors. Although occupancy may seem quasi-static (around class timetables), it is dynamic and closely tied to human behavior: opening and closing of windows and doors, exhalation variability depending on activity levels, and informal or unscheduled use of spaces. The second approach relates to architectural characteristics. Despite their static appearance, show dynamic effects through their interaction with external climate, thermal inertia, and HVAC operation. These interactions condition how each building behaves over time and how human dynamics manifest across spatial configurations. The combination of both dimensions (occupancy and architecture) highlights that IAQ behavior is inherently complex. As summarized contribution from the following key findings, this paper advances several data-driven strategies as intervention proposals for new CO_2-based deployments, such as:

- Select the most suitable classroom for each subject according to key factors (orientation, location, and size).
- Assign highest occupancy subjects to best orientation spaces (north/south–facing) with lowest CO_2 levels.
- Perform weekly analysis to obtain day-pattern guides for CO_2-based ventilation in the following weeks.

These examples of decision-making under real conditions constitute as preliminary step for further algorithms and models toward efficient management of IAQ and HVAC. As quantitative estimation, these intervention proposals result in an average saving of around €500 in 1 month in one building [21]. This estimated saving, extrapolated to every month during the study period of the three buildings, would be around €7500. Replicating these data-driven strategies to tertiary building is very indicative of their economic impact. Furthermore, as the following insights show, an efficient CO_2-based ventilation could enhance IAQ between 3% and 10% regarding occupancy patterns and space sizes, and between 4% and 13% regarding orientation and location.

From the obtained results, the key findings highlight how indoor CO_2 behavior under real conditions combines influence of occupancy patterns, space size, and contextual factors, with the following insights:

- Occupancy and size. Higher CO_2 levels correlate strongly with increases in occupancy and the duration of such occupancy, making these variables the most influential contributors across the monitored spaces. With low occupancy, CO_2 remains below 1000 ppm for more than 95% of time, whereas in moderate-occupancy spaces this percentage decreases by 1%–5%. With high occupancy, this percentage decreases progressively with size, averaging 90% in large spaces, 87% in medium spaces and 80% in small spaces. These results show how the interaction between size and occupancy intensity shapes CO_2 accumulation patterns.
- Size, occupancy and CO_2 evolution: Larger spaces (or small spaces with low and variable occupancy) remain $CO_2 < 1000$ ppm for more than 95% of the time, with improvements of 1%–2% when occupancy is low rather than moderate. Comparing medium-size spaces with moderate occupancy to large spaces with high occupancy, IAQ improves between 4%–10% (for $CO_2 < 800$ ppm) and 3%–5% (for $CO_2 < 1000$ ppm). These patterns intensify during months with greater teaching activity (particularly November, followed by October and December) producing a characteristic triangular pattern. In small and high-occupancy spaces (labs), this effect is even more pronounced with $CO_2 > 1000$ ppm for 15%–27% of monitored time, and $CO_2 > 1500$ ppm for 5%–9%, following human factor of interactions for team-based practical sessions.
- Contextual factors: CO_2 behavior is dynamic and context-dependent: architectural features interact with climatic conditions, HVAC operation and human behavior, producing patterns that evolve over time. Before studying specific trends, it is key to consider how these elements combine to affect natural ventilation, modulate thermal comfort, and determine how CO_2 varies in different spaces regarding three aspects.

- A first aspect concerns orientation and climatic conditions: In medium-size spaces with moderate occupancy, CO_2 concentrations rise progressively as outdoor temperatures fall, largely because occupants do not open windows or doors during colder months. This behavior leads to seasonal patterns: comparing north- and south-facing spaces, $CO_2 > 1000$ ppm consistently decreases in south-facing spaces: from 5% to 2% (September), from 9% to 5% (October), from 11% to 7% (November), and from 13% to 10% (December). South-facing spaces benefit from high solar exposure, which encourages natural ventilation, whereas north-facing spaces tend to keep windows closed for thermal comfort, increasing $CO_2 > 1500$ ppm by 1%–2%.
- A second aspect relates to location: Under the same conditions (large size and high-occupancy), $CO_2 > 1000$ ppm on the Floor 0 (typically colder and less prone to natural ventilation) increases by 4%–6% compared with upper floors. This due reinforces the orientation and location as key contextual factors.
- Finally, spaces with variable occupancy reveal the strongest expression of human dynamics. Continuous entries and exits, frequent door opening and inconsistent window use create fluctuating ventilation patterns. In large and well-ventilated canteens, size itself does not significantly condition IAQ; however, $CO_2 > 1000$ ppm in a medium-size canteen (Building A) increases by 3% compared with a larger one (Building C). In the library (a large and quiet environment) the relationship becomes even clearer: CO_2 levels remain low, with $CO_2 > 1000$ ppm around 10%, as most occupants are studying silently, producing minimal exhalation and allowing ventilation to remain effective.

From these insights, CO_2 dynamics have been analyzed from two complementary perspectives:

- At the day-by-day scale, the analysis provides an overarching view of how CO_2 evolves throughout the week, helping to identify structural patterns in IAQ behavior. Daily maximum CO_2 values make it possible to calibrate the reference baseline (around 420 ppm), mark the beginning and end of each week (five school days followed by two weekend days), and detect nonworking days or holiday periods. This temporal overview offers an initial, data-driven interpretation of IAQ patterns and detects critical high-CO_2 situations. Therefore, this day-scale perspective offers a valuable tool for anticipating ventilation needs and planning preventive IAQ actions at the building-management level.
- At the hour-by-hour scale, CO_2 evolution shows fine-tuning dynamics associated with class schedules, occupancy cycles and breaks between sessions. Obtained results in a set of five school days can estimate ACH during class transitions for 1 h (CO_2 decreases in Day 3 from 1100 to 550 ppm between 11 h and 12 h, and from 850 to 450 ppm between 14 h and 15 h). During shorter breaks between consecutive classes (when doors and windows are briefly open), CO_2 decays from 850 to 600 ppm (1 ACH on Day 2), and from 1000 to 750 ppm (1 ACH on Day 3). After the end of classes, CO_2 evolution enables quantification of decay rates, showing a nonlinear trend that could be parameterized quantitatively in future research. This hour-scale perspective provides operational insight into how quickly spaces recover ventilation effectiveness, informing decisions related to class scheduling, window-opening protocols, and HVAC adjustments.

In summary, all these contributions move toward understanding IAQ in its dynamic complexity under real conditions in large-scale infrastructures. Through a real-time monitoring IoT ecosystem, this paper proposes methodological procedures through campus-wide deployments to multifaceted parameterize CO_2 behavior by its dynamic components: variability of occupancy, architectural context, temporal evolution, unpredictability of human activity, among other context factors. As a result, these experimental insights can be extrapolated to multiple context-aware approaches for IAQ management and planning in tertiary buildings.

Nomenclature

ACH	air changes per hour
BPG	building performance gap
HVAC	heating, ventilation, and air conditioning
IAQ	indoor air quality
IEQ	indoor environmental quality
IoT	Internet of Things
LoRaWAN	low-range wide-area network
LP-WAN	low-power wide-area network
NDIR	nondispersive infrared
PM	particulate matters
SBE	Smart Built Environment
VOC	volatile organic compounds

Funding

This study was supported by the Gobierno de Aragón (10.13039/501100010067) (420, T27_23R).

Conflicts of Interest

The authors declare no conflicts of interest.

Data Availability Statement

The data that support the findings of this study are openly available in sensoriZAR UZ smart campus at https://eina.unizar.es/sensorizar.

References

1. S. Ahmed, A. Pasha, T. Kumer, M. Akhtaruzzaman, and M. Hossain, "Advancements in Air Quality Monitoring Systems: A Comprehensive Review of Emerging Technologies for Enhancing Environmental Health," *Indoor Air* 2026, no. 1 (2026): 3080684, https://doi.org/10.1155/ina/3080684.

2. World Health Organization (WHO), *WHO Global Air Quality Guidelines: Particulate Matter (PM2.5 and PM10), Ozone, Nitrogen Dioxide, Sulfur Dioxide and Carbon Monoxide* (World Health Organization (WHO), 2021), https://www.who.int/publications/i/item/9789240034228.

3. Environmental Protection Agency (EPA), *Why Indoor Air Quality Is Important to Schools* (Environmental Protection Agency (EPA), 2025), https://www.epa.gov/iaq-schools/why-indoor-air-quality-important-schools.

4. World Health Organization (WHO), *Air Quality, Energy and Health. Types of Pollutants* (World Health Organization (WHO), 2025), https://www.who.int/teams/environment-climate-change-and-health/air-quality-and-health/health-impacts/types-of-pollutants.

5. S. Park, and D. Song, "CO2 Concentration as an Indicator of Indoor Ventilation Performance to Control Airborne Transmission of SARS-CoV-2," *Journal of Infection and Public Health* 16, no. 7 (2023): 1037–1044, https://doi.org/10.1016/j.jiph.2023.05.011.

6. La Asociación Española de Normalización, "Energy Performance of Buildings - Ventilation for Buildings - Part 1:," in *Indoor Environmental Input Parameters for Design and Assessment of Energy Performance of Buildings Addressing Indoor Air Quality, Thermal Environment, Lighting and Acoustics - Module M1-6* (La Asociación Española de Normalización, 2020), https://www.une.org/encuentra-tu-norma/busca-tu-norma/norma?c=N0063261.

7. European Union, "Directive 2008/50/EC of the European Parliament and of the Council of 21 May 2008 on Ambient Air Quality and Cleaner Air for Europe," *Official Journal of the European Union* 152 (2008): 1–44, https://eur-lex.europa.eu/eli/dir/2008/50/oj/eng.

8. European Commission, *Technical Study on the Possible Introduction of Inspection of Stand-Alone Ventilation Systems in Buildings* (Publications Office of the European Union, 2020), https://data.europa.eu/doi/10.2833/621790.

9. American Society of Heating, Refrigerating and Air-Conditioning Engineers, *Position Document on Indoor Carbon Dioxide* (American Society of Heating, Refrigerating and Air-Conditioning Engineers, 2022), https://Www.Ashrae.Org/File%2520library/about/Position%2520documents/Pd-on-Indoor-Carbon-Dioxide-English.Pdf.

10. United Nations, *Sustainable Development Goals (SDG)* (United Nations, 2025), https://www.un.org/sustainabledevelopment.

11. World Health Organization (WHO), *Guidelines for Indoor Air Quality: Selected Pollutants* (World Health Organization (WHO), 2010), https://www.who.int/publications/i/item/9789289002134.

12. Environmental Protection Agency (EPA), *2012 National Ambient Air Quality Standards (NAAQS) for Particulate Matter (PM)* (Environmental Protection Agency (EPA), 2012), https://www.epa.gov/pm-pollution/2012-national-ambient-air-quality-standards-naaqs-particulate-matter-pm.

13. World Health Organization (WHO), *WHO Global Air Quality Guidelines: Particulate Matter, Ozone, Nitrogen Dioxide, Sulfur Dioxide and Carbon Monoxide* (World Health Organization (WHO), 2021), https://www.who.int/publications/i/item/9789240034228.

14. D. Marín, A. Alegría-Sala, L. Canals, M. Macarulla, and J. Fonollosa, "The Reliability of CO2 Measurements Using Low-Cost Sensors: A Study of Sensor Positioning and Ventilation Strategies in Classrooms," *Indoor Air* 2025, no. 1 (2025): 5517242, https://doi.org/10.1155/ina/5517242.

15. L.-R. Jia, J. Han, X. Chen, Q.-Y. Li, C.-C. Lee, and Y.-H. Fung, "Interaction Between Thermal Comfort, Indoor Air Quality and Ventilation Energy Consumption of Educational Buildings: A Comprehensive Review," *Buildings* 11, no. 12 (2021): 591, https://doi.org/10.3390/buildings11120591.

16. A. Persily, "Development and Application of an Indoor Carbon Dioxide Metric," *Indoor Air* 32, no. 7 (2022): e13059, https://doi.org/10.1111/ina.13059.

17. Á. Muelas, P. Remacha, A. Pina, et al., "Analysis of Different Ventilation Strategies and CO2 Distribution in a Naturally Ventilated Classroom," *Atmospheric Environment* 283 (2022): 119176, https://doi.org/10.1016/j.atmosenv.2022.119176.

18. A. Franco, E. Crisostomi, F. Leccese, A. Mugnani, and S. Suin, "Energy Savings in University Buildings: The Potential Role of Smart Monitoring and IoT Technologies," *Sustainability* 17, no. 1 (2025): 111, https://doi.org/10.3390/su17010111.

19. A. Zivelonghi, and P. Kumar, "Benefits and Thermal Limits of CO_2-Driven Signaled Windows Opening in Schools: An In-Depth Data-Driven Analysis," *Energy and Buildings* 303 (2024): 113621, https://doi.org/10.1016/j.enbuild.2023.113621.

20. C. Ren, H.-C. Zhu, J. Wang, et al., "Intelligent Operation, Maintenance, and Control System for Public Building: Towards Infection Risk Mitigation and Energy Efficiency," *Sustainable Cities and Society* 93 (2023): 104533, https://doi.org/10.1016/j.scs.2023.104533.

21. I. Martínez, E. Cano-Suñén, R. Casas, and Á. Fernández, "Smart Built Environment (SBE): A Challenge for Internet of Things (IoT) Ecosystems to Understand Dynamic Habitats and Their Users as Complex Systems," *Journal of Building Engineering* 116 (2025): 114620, https://doi.org/10.1016/j.jobe.2025.114620.

22. M. Taştan, "Machine Learning–Based Calibration and Performance Evaluation of Low-Cost Internet of Things Air Quality Sensors," *Sensors* 25, no. 10 (2025): 3183, https://doi.org/10.3390/s25103183.

23. M. T. Bashir, R. Alrowais, R. Lal, et al., "Synergizing Health and Technology in Green Buildings: A Critical Review of Indoor Air Quality Monitoring and Solutions," *Indoor Air* 2025, no. 1 (2025): 1281155, https://doi.org/10.1155/ina/1281155.

24. T. Heemstra, M. van der Schans, J. Gibas, J.-P. M. G. Linnartz, and R. Delnoij, "Ceiling-Mounted CO 2 Sensing: Effect of Location and Stratification Temperature," *Indoor Air* 2024, no. 1 (2024): 1840021, https://doi.org/10.1155/2024/1840021.

25. C. Avila, P. Tapia, R. Vallejo, A. Avila, and E. Rivera, "In Pursuit of Healthier Learning Environments: High-Altitude Classroom Ventilation," *Indoor Air* 2024, no. 1 (2024): 2205311, https://doi.org/10.1155/2024/2205311.

26. Z. Huang, H. Zhou, Z. Miao, H. Tang, B. Lin, and W. Zhuang, "Life-Cycle Carbon Emissions (LCCE) of Buildings: Implications, Calculations, and Reductions," *Engineering* 35, no. 4 (2024): 115–139, https://doi.org/10.1016/j.eng.2023.08.019.

27. B. F. Marfo, F. K. Bondinuba, and C. M. Mewomo, "A Theoretical Framework Towards Leveraging Internet of Things Applications in Building Energy Efficiency," *Property Management* 44, no. 2 (2026): 1–24, https://doi.org/10.1108/PM-04-2025-0051.

28. E. Mousavi, A. Bhattacharya, F. Betz, and R. Lautz, "Evolution of Ventilation Measures and Energy Performance in Buildings With High Ventilation Demands: A Critical Review," *Energies* 18, no. 14 (2025): 3603, https://doi.org/10.3390/en18143603.

29. Y. Wei, S. Wang, L. Jin, Y. Xu, and T. Ding, "Indoor Occupancy Estimation From Carbon Dioxide Concentration Using Parameter Estimation Algorithms," *Building Services Engineering Research and Technology* 43, no. 4 (2022): 419–438, https://doi.org/10.1177/01436244211060903.

30. H. P. Oswin, L. Glachant, S. A. Lekamge, B. Alinaghipour, S. B. Khan, and L. Morawska, "Using Indoor CO2 Concentration Thresholds to Understand and Improve the Air Quality of Public Buildings: A Practical Approach," *Energy and Buildings* 347 (2025): 116254, https://doi.org/10.1016/j.enbuild.2025.116254.

31. B. Chenari, S. Saadatian, and M. Gameiro da Silva, "Experimental Assessment of Demand-Controlled Ventilation Strategies for Energy Efficiency and Indoor Air Quality in Office Spaces," *Air* 3, no. 2 (2025): 17, https://doi.org/10.3390/air3020017.

32. X. Lu, Z. Pang, Y. Fu, and Z. O'Neill, "Advances in Research and Applications of CO2-Based Demand-Controlled Ventilation in Commercial Buildings: A Critical Review of Control Strategies and Performance Evaluation," *Building and Environment* 223 (2022): 109455, https://doi.org/10.1016/j.buildenv.2022.109455.

33. J. Gao, M. Yu, Y. Xu, et al., "Use of Wearable Ventilation for Reducing the Infection Risk of Healthcare Workers in Isolation Wards: A Numerical Study," *Building and Environment* 265 (2024): 112019, https://doi.org/10.1016/j.buildenv.2024.112019.

34. I. Cimbru, J. Wagner, and A. Zeier Röschmann, "On IoT-Enabled Risk Prevention and Insurance: A Systematic Literature Review," *Risk Management and Insurance Review* 28, no. 4 (2025): 643–694, https://doi.org/10.1111/rmir.70025.

35. P. Gasbarri, S. Meschini, L. C. Tagliabue, and G. M. Di Giuda, "Users' Well-Being in University Buildings: Towards a Research Framework Development," *Journal of Physics: Conference Series* 3140, no. 9 (2025): 092008, https://doi.org/10.1088/1742-6596/3140/9/092008.

36. K. Przystupa, N. Bernatska, E. Dzhumelia, T. Drzymała, and O. Kochan, "Ensuring Energy Efficiency of Air Quality Monitoring Systems Based on Internet of Things Technology," *Energies* 18, no. 14 (2025): 3768, https://doi.org/10.3390/en18143768.

37. I. Martínez, B. Zalba, R. Trillo-Lado, T. Blanco, D. Cambra, and R. Casas, "Internet of Things (IoT) as Sustainable Development Goals (SDG) Enabling Technology Towards Smart Readiness Indicators (SRI) for University Buildings," *Sustainability* 13, no. 14 (2021): 7647, https://doi.org/10.3390/su13147647.

38. E. Cano-Suñén, I. Martínez, Á. Fernández, B. Zalba, and R. Casas, "Internet of Things (IoT) in Buildings: A Learning Factory," *Sustainability* 15, no. 16 (2023): 12219, https://doi.org/10.3390/su151612219.

39. F. A. Wani, V. Sharma, A. Pal, S. Mathur, and J. Mathur, "Occupant Centric Indoor Environmental Quality (IEQ) Assessment Within Institutional Settings," *Smart and Sustainable Built Environment* (2026): 1–25, Vol. ahead-of-print No. ahead-of-print, https://doi.org/10.1108/SASBE-05-2025-0238.

40. K. Rastogi, and D. Lohani, "Context-Aware IoT-Enabled Framework to Analyse and Predict Indoor Air Quality," *Intelligent Systems With Applications* 16 (2022): 200132, https://doi.org/10.1016/j.iswa.2022.200132.

41. A. Katal, L. L. Wang, and M. Albettar, "A Real-Time Web Tool for Monitoring and Mitigating Indoor Airborne COVID-19 Transmission

Risks at City Scale," *Sustainable Cities and Society* 80 (2022): 103810, https://doi.org/10.1016/j.scs.2022.103810.

42. A. Franco, E. Crisostomi, A. Sodini, M. Tili, and A. Mugnani, "Integrating Energy Efficiency and Occupancy Control in Shared Public Buildings: A Data-Driven Approach," *Mathematical Modelling and Engineering Problems* 11, no. 10 (2024): 2695–2704, https://doi.org/10.18280/mmep.111011.

43. M. Justo Alonso, S. Wolf, R. B. Jørgensen, H. Madsen, and H. M. Mathisen, "A Methodology for the Selection of Pollutants for Ensuring Good Indoor Air Quality Using the De-Trended Cross-Correlation Function," *Building and Environment* 209 (2022): 108668, https://doi.org/10.1016/j.buildenv.2021.108668.

44. Universidad Zaragoza, *UZ Smart Campus. University of Zaragoza (UZ) IoT Ecosystem* (Universidad Zaragoza, 2025), https://sensouz.unizar.es (see also https://eina.unizar.es/sensorizar).

45. S.-C. Qi, Z. Sun, Z.-H. Yang, et al., "Photo-Responsive Carbon Capture over Metalloporphyrin-C 60 Metal-Organic Frameworks via Charge-Transfer," *Research* 6 (2023): 0261, https://doi.org/10.34133/research.0261.

46. R. Dubey, A. Telles, J. Nikkel, et al., "Low-Cost CO2 NDIR Sensors: Performance Evaluation and Calibration Using Machine Learning Techniques," *Sensors* 24, no. 17 (2024): 5675, https://doi.org/10.3390/s24175675.

47. N. Mohtashami, N. Sauer, R. Streblow, and D. Müller, "Comparative Analysis of Smart Building Solutions in Europe: Technological Advancements and Market Strategies," *Energies* 18, no. 3 (2025): 682, https://doi.org/10.3390/en18030682.

48. SanityAir, *CO2 Monitors* (SanityAir, 2025), https://sanity-air.com/en/producto/air-experience-2.

49. Milesight, *CO2 Monitors AM307/308/319* (Milesight, 2025), https://www.milesight.com/iot/product/lorawan-sensor/am319.

50. Aranet, *CO2 Monitors Home/Pro* (Aranet, 2025), https://www.aranet4.es.

51. Dienmern, *DM. CO2 Monitors* (Dienmern, 2025), https://www.dienmern-instrument.com/latest-carbon-dioxide-detector.html.

52. Globalia Protección, *CO2Panel CO2 Monitors PI/Matrix* (Globalia Protección, 2025), https://globaliaproteccion.com/tienda/producto/medidor-concentracion-de-co2-panelpi.

53. Quantum, *Dioxcare. CO2 Monitors* (Quantum, 2025), https://quantumspain.es/medidores-de-calidad-del-aire/medidor-de-co2-portatil-dioxcare-dx700-pdf.html.

54. LoRa Alliance, *What is LoRaWAN Specification* (LoRa Alliance, 2025), https://lora-alliance.org/about-lorawan.

55. Testo, *Testo 480. Certified Calibration Device* (Testo, 2025), https://www.testo.com/es-ES/instrumento-multi-parametro-testo-480/p/0563-4800.